Advanced Piezoelectric crystals of $La_3Ga_5SiO_{14}$ Family

D.V. Roshchupkin, O.A. Plotitcyna

Institute of Microelectronics Technology and High-Purity Materials
Russian Academy of Sciences

Plan of presentation

1. Advanced piezoelectric crystals for acoustoelectronics
2. Crystal structure perfection
3. Independent piezoelectric strain coefficients (d_{11}, d_{14}) in $La_3Ga_{5.3}Ta_{0.5}Al_{0.2}O_{14}$ and $Ca_3TaGa_3Si_2O_{14}$ crystals
4. QCM Microbalance based on LGTA crystal
5. High temperature wireless sensor based on surface acoustic waves resonators (-90ºC ÷ 1000ºC, LGS: $La_3Ga_5SiO_{14}$)
6. Fast X-Ray beam chopper
7. SAW imaging by Talbot effect at the synchrotron radiation source
8. Ordering $Ca_3TaGa_3Si_2O_{14}$ crystal
9. Non-ordering $La_3Ga_{5.3}Ta_{0.5}Al_{0.2}O_{14}$ crystal
10. Investigation of surface and pseudo-surface acoustic waves excitation and propagation in $La_3Ga_5SiO_{14}$ crystal

1. Advanced piezoelectric crystals for acoustoelectronics

Crystals of $La_3Ga_5SiO_{14}$ (LGS, langasite) family, point group symmetry 32

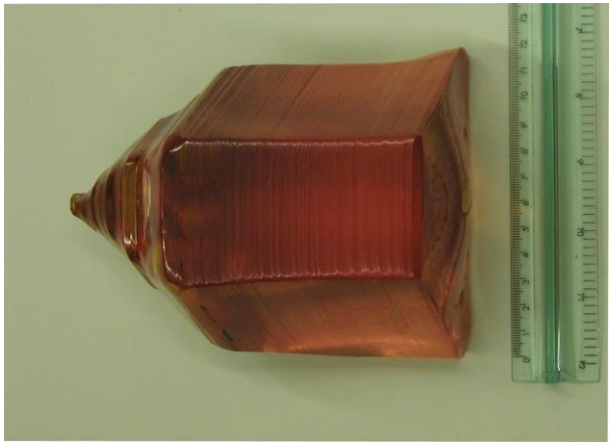

4" non-ordering $La_3Ga_5SiO_{14}$ crystal grown along axis {001}

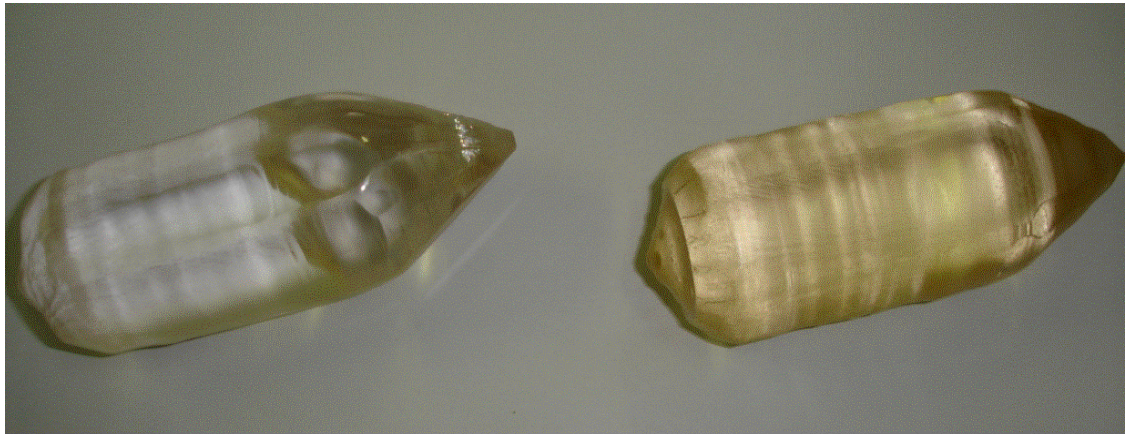

3" ordering $Ca_3TaGa_3Si_2O_{14}$ crystal grown along axis {110}

3" non-ordering $La_3Ga_{5.5}Ta_{0.5}O_{14}$ crystal grown along axis {001}

3" non-ordering $La_3Ga_{5.5}Ta_{0.3}Al_{0.2}O_{14}$ crystal grown along axis {110}

2. Crystal structure perfection

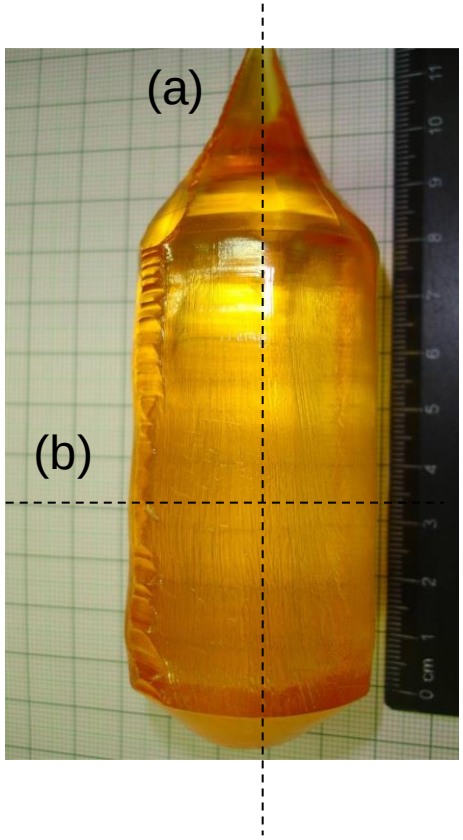

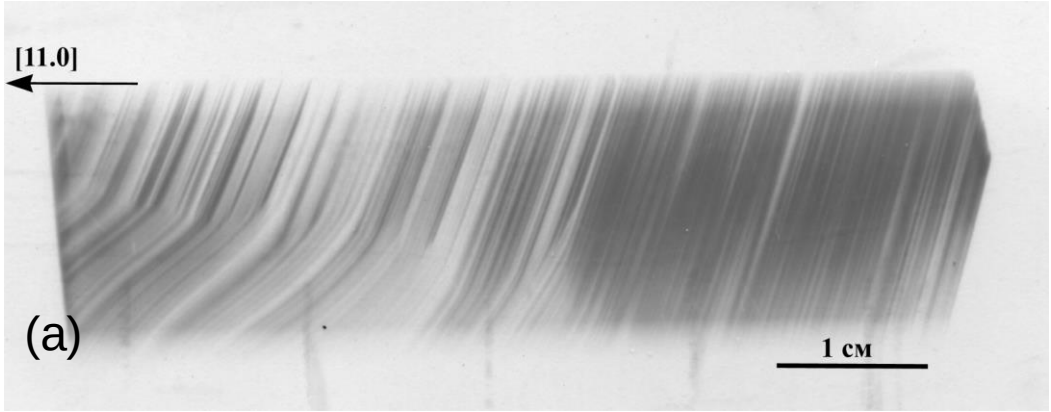

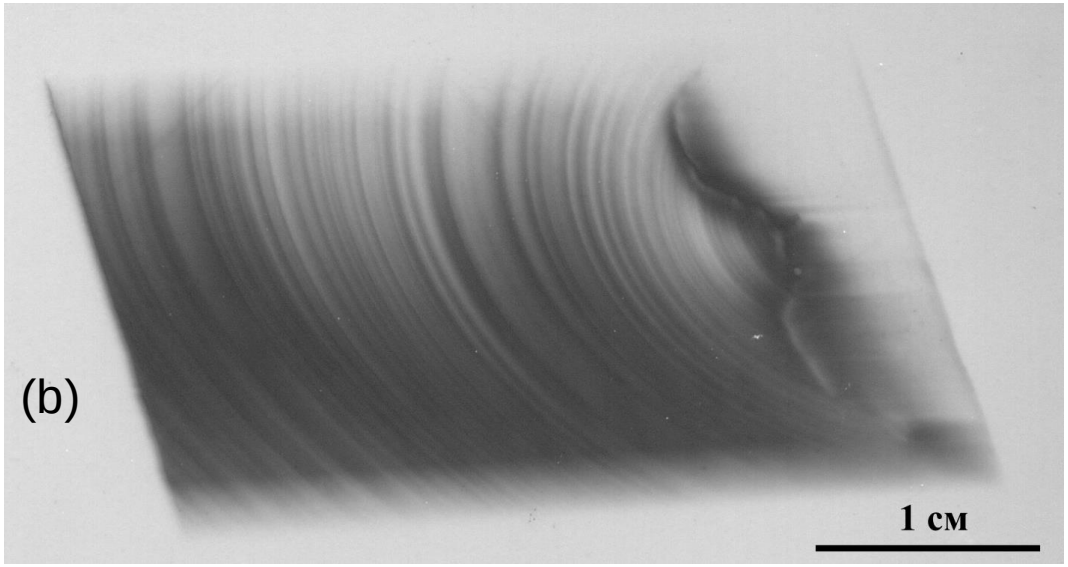

X-ray topographs of LGTA:
(a) reflection (003), Θ_B=21.901º, λ=1.276 Å;
(b) reflection (220), Θ_B=17.836º, λ=1.276 Å.

Measurements of interplanar spacing in LGTA crystal

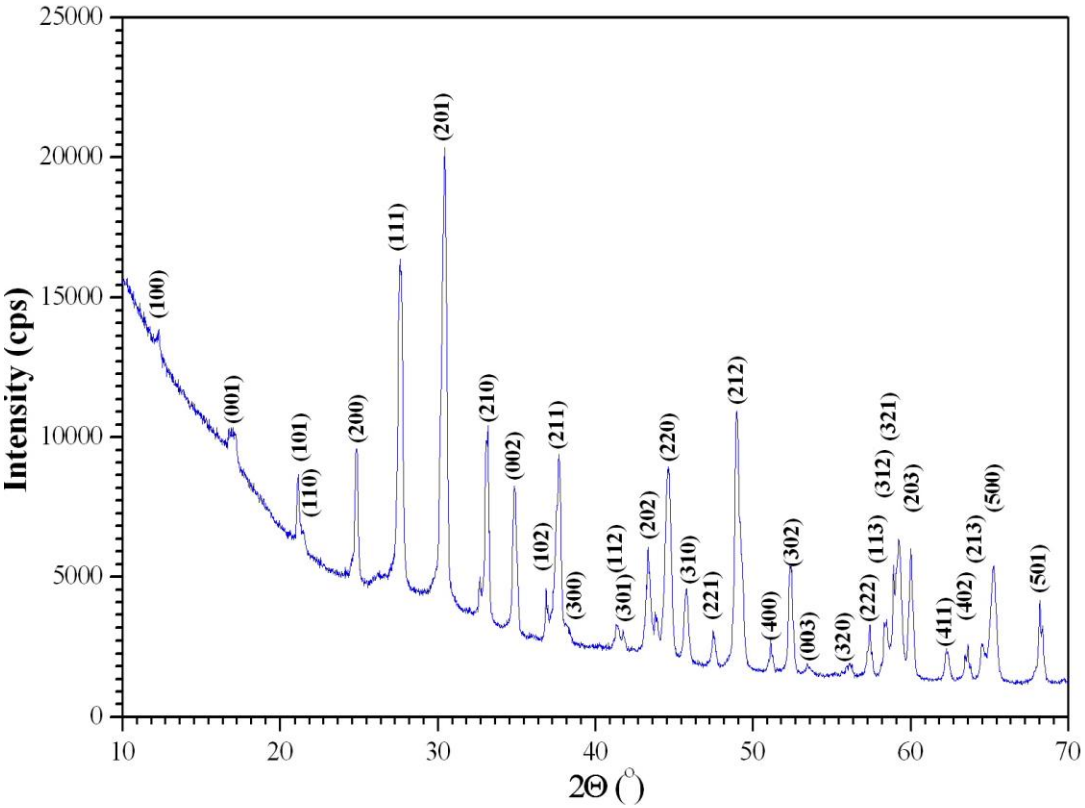

XRD diffraction spectrum of LGTA crystal

Reflection (hkl)	2Θ, º	$d_{(hkl)}$, Å
(100)	12,2438	7,2203
(001)	16,9112	5,2366
(110)	21,4094	4,1454
(200)	24,8491	3,5788
(111)	27,6327	3,2243
(201)	30,4162	2,9353
(210)	33,1152	2,7020
(002)	34,8404	2,5720
(300)	38,3648	2,3434
(112)	41,3918	2,1788
(202)	43,4344	2,0809
(220)	44,6199	2,0283
(310)	45,8188	1,9780
(221)	47,5304	1,9107
(212)	48,9275	1,8594
(400)	51,2136	1,7816
(302)	52,4413	1,7427
(003)	53,5103	1,7104
(222)	57,4369	1,6025
(321)	59,2362	1,5580
(203)	60,0617	1,5384
(402)	63,6603	1,4600
(500)	65,3007	1,4272
(501)	68,1670	1,3740

$a=b=2d_{(110)}=8.2908$ Å

$c=2d_{(002)}=5.144$ Å

3. Independent piezoelectric strain coefficients (d_{11}, d_{14}) in $La_3Ga_{5.3}Ta_{0.5}Al_{0.2}O_{14}$ (LGTA) and $Ca_3TaGa_3Si_2O_{14}$ (CTGS) crystals

Reverse piezoelectric effect : $\Delta d_i/d_i = d_{ij} \cdot E_j$

X-cut of the LGTA crystal, thickness 200 μm

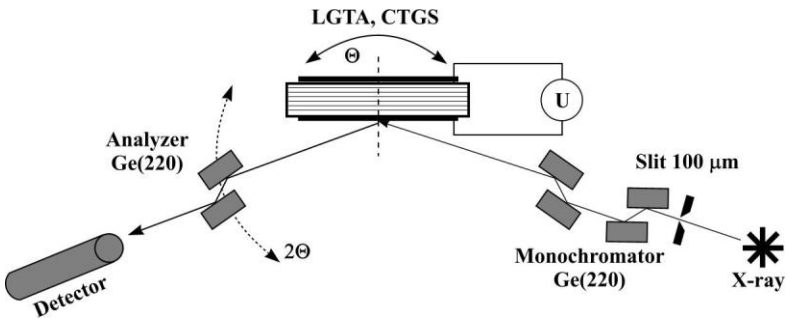

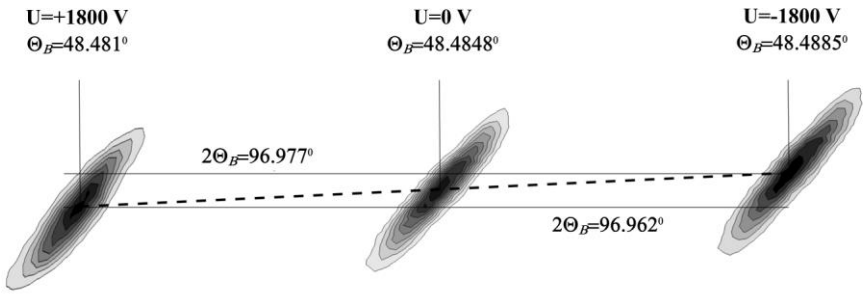

Measurements of d_{11} in the Bragg diffraction geometry.
Reflection (110). d_{11}=6.45455×10^{-12} C/N

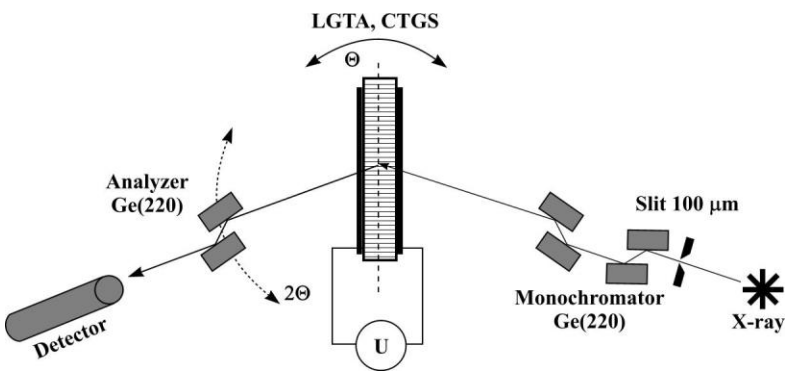

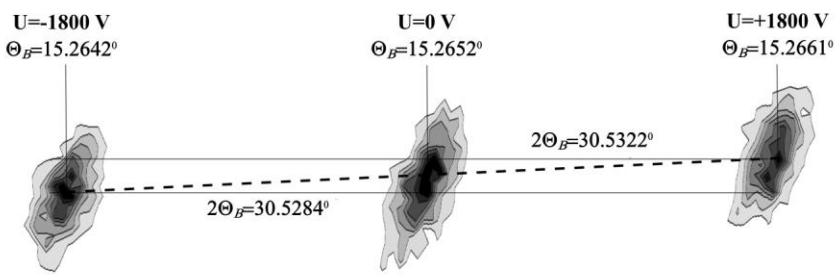

Measurements of d_{14} in the Laue diffraction geometry.
Reflection (201). d_{14}=–5.11735×10^{-12} C/N

Piezoelectric strain coefficients d_{11} and d_{14} in LGTA and CTGS crystals

References	$La_3Ga_{5.3}Ta_{0.5}Al_{0.2}O_{14}$ (LGTA)		$Ca_3TaGa_3Si_2O_{14}$ (CTGS)	
	$d_{11}\times10^{-12}$ (C/N)	$d_{14}\times10^{-12}$ (C/N)	$d_{11}\times10^{-12}$ (C/N)	$d_{14}\times10^{-12}$ (C/N)
Ref. 1	6.6	-	-	-
Ref. 2	-	-	-4.58	10.43
Ref. 3	6.455	-5.117	3.331	-15.835

1. Shujun Zhang, Akira Yoshikawa, Kei Kamada, Eric Frantz, Ru Xia, David W. Snyder, Tsuguo Fukuda, and Thomas R. Shrout, "Growth and characterization of high temperature $La_3Nb_{0.5}Ga_{5.3}Al_{0.2}O_{14}$ (LNGA) and $La_3Ta_{0.5}Ga_{5.3}Al_{0.2}O_{14}$ (LTGA) piezoelectric single crystals," Solid State Comm. **148** 213 (2008).
2. Xuzhong Shi, Duorong Yuan, Xin Yin, Aijian Wei, and Shiyi Guo, Fapeng Yu, "Crystal growth and dielectric, piezoelectric and elastic properties of $Ca_3TaGa_3Si_2O_{14}$ single crystal," Solid State Comm. **142** 173 (2007).
3. Dmitry Irzhak and Dmitry Roshchupkin, Piezoelectric strain coefficients in $La_3Ga_{5.3}Ta_{0.5}Al_{0.2}O_{14}$ and $Ca_3TaGa_3Si_2O_{14}$ crystals, AIP Advanced (2013).

4. QCM Microbalance based on LGTA crystal

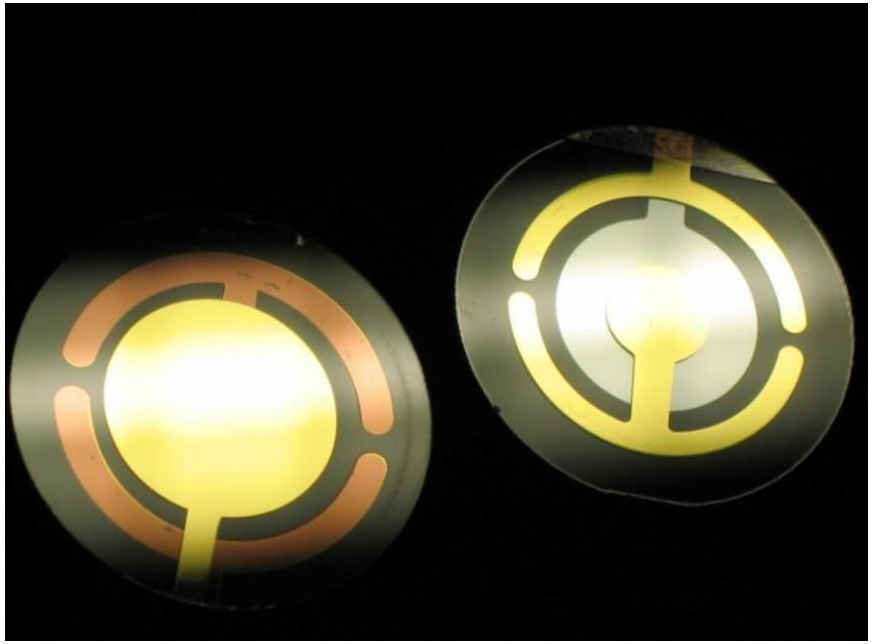

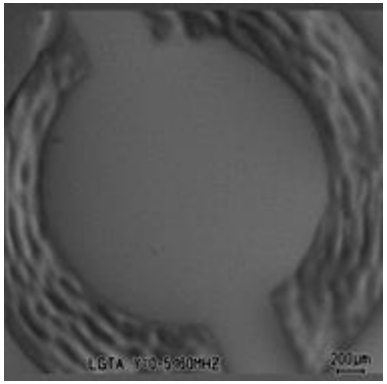

LGTA *Y*-cut, (100), f_0=5.160 МГц

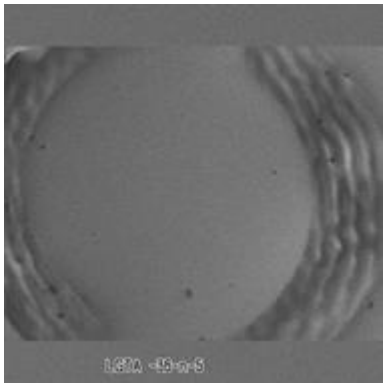

LGTA *Y*-36º-cut, (101), f_0=4.490 МГц

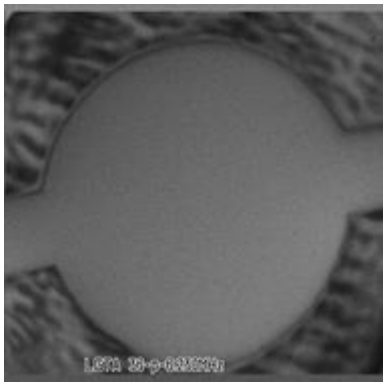

LGTA *Y*+36º-cut, (101), f_0=6.230 МГц

Application of QCM Microbalance:

- Control of the thickness of refractory films in industry;
- Control of the thickness of an epitaxial growth films in micro- and nanoelectronics;
- Monitoring of high-temperature processes;
- Control of hydrogen concentration at the Nuclear Power Plant.

QCM BAW-resonators

LGTA *Y*-cut, (100)

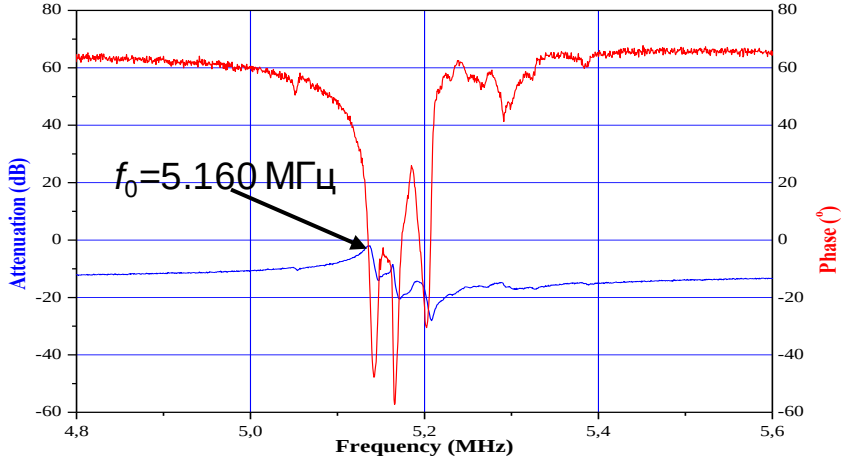

Amplitude-frequency response

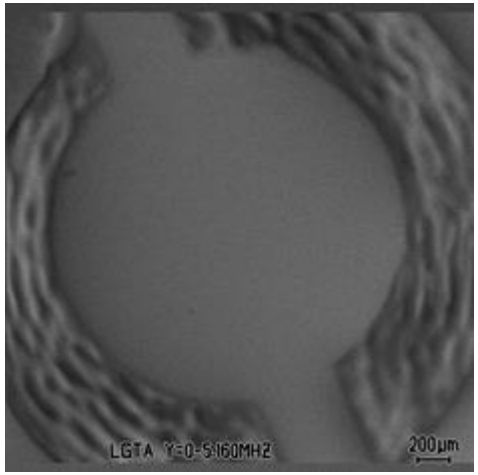

BAW-resonator, f_0=5.160 MHz

LGTA *Y*+36º-cut, (101)

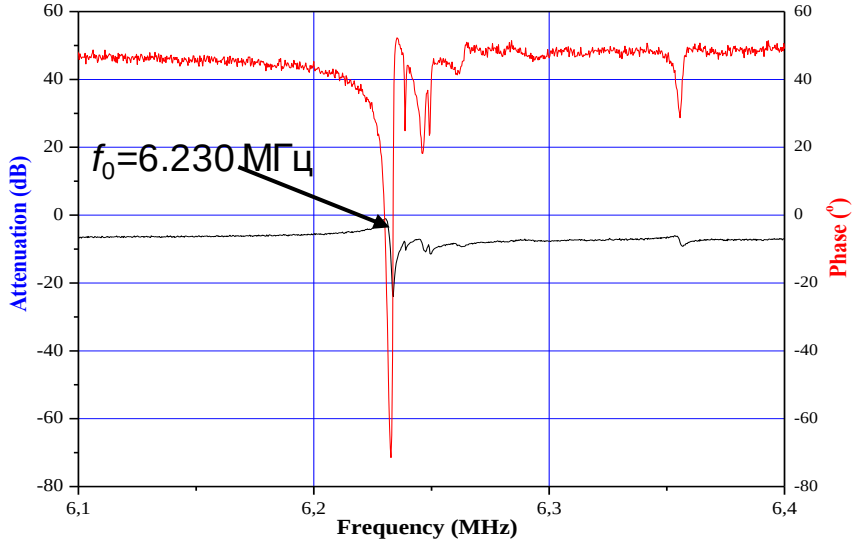

Amplitude-frequency response

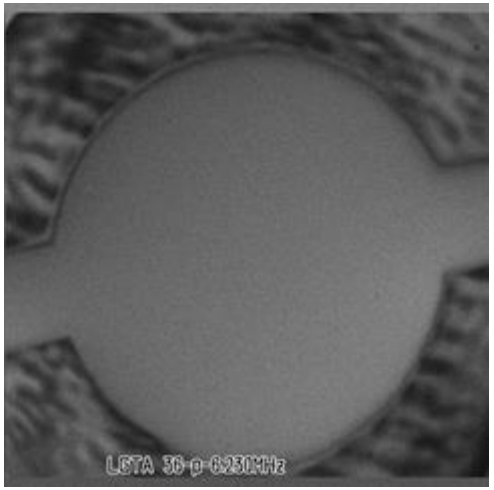

BAW-resonator, f_0=6.230 MHz

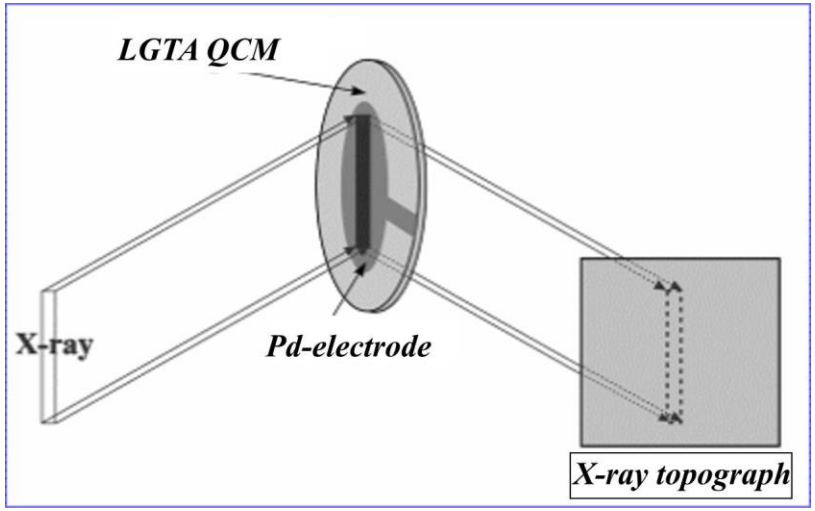

Experimental set-up of X-ray topograph.

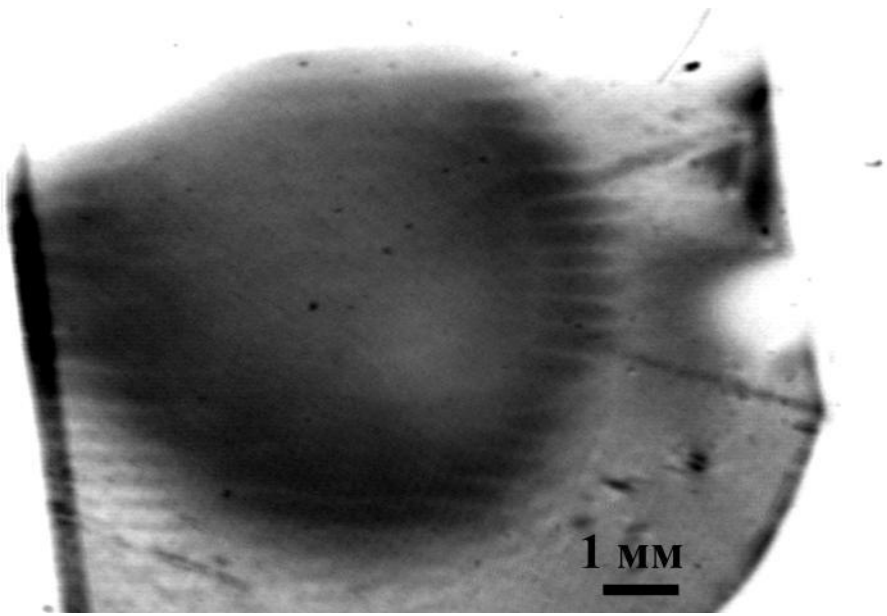

X-ray topograph of the QCM based on *yxl*/-36º-cut of an LGTA crystal.
Reflection (201), Θ_B=6.199º, *f*=6.1076 MHz.

5. High temperature wireless sensor based on surface acoustic waves resonators (-90ºC ÷ 1000ºC, LGS: $La_3Ga_5SiO_{14}$)

SAWHOT
Wireless SAW sensor for high temperature

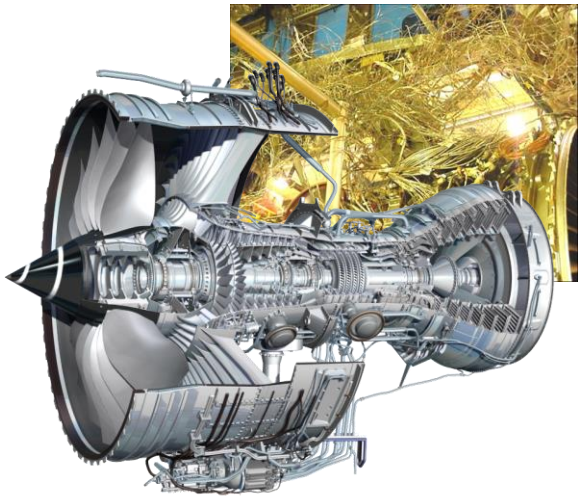

Aero-engine

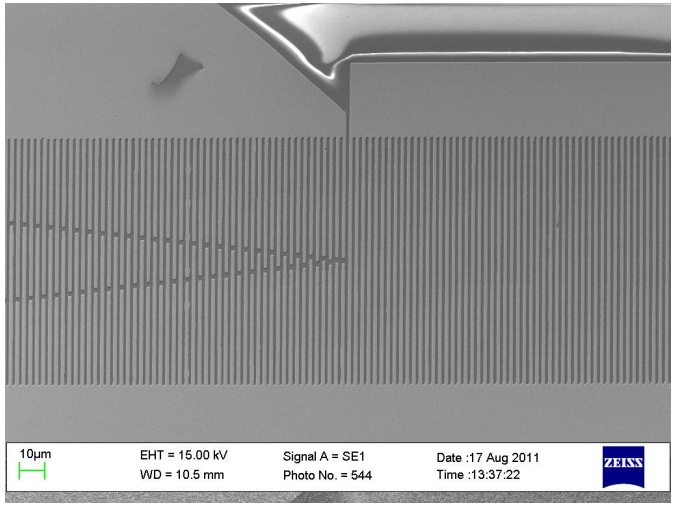

Ir-IDT (Λ=5.948 µm)

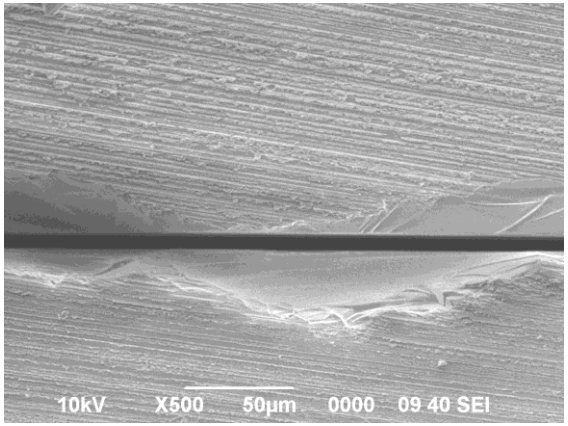

Package: LGS

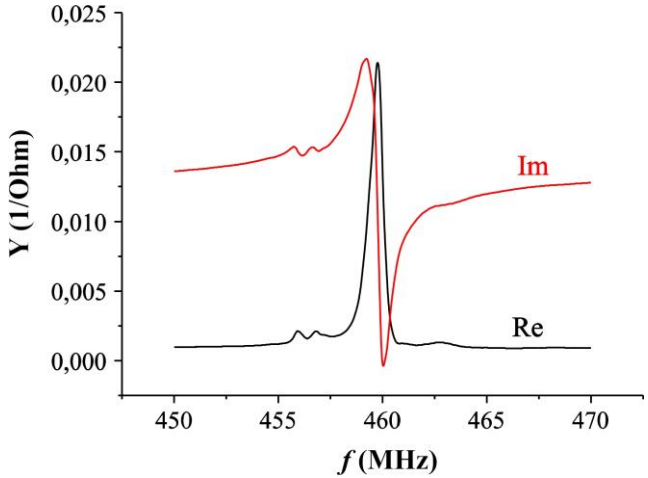

Amplitude-frequency response of SAW-resonator

Y-cut of LGS crystal

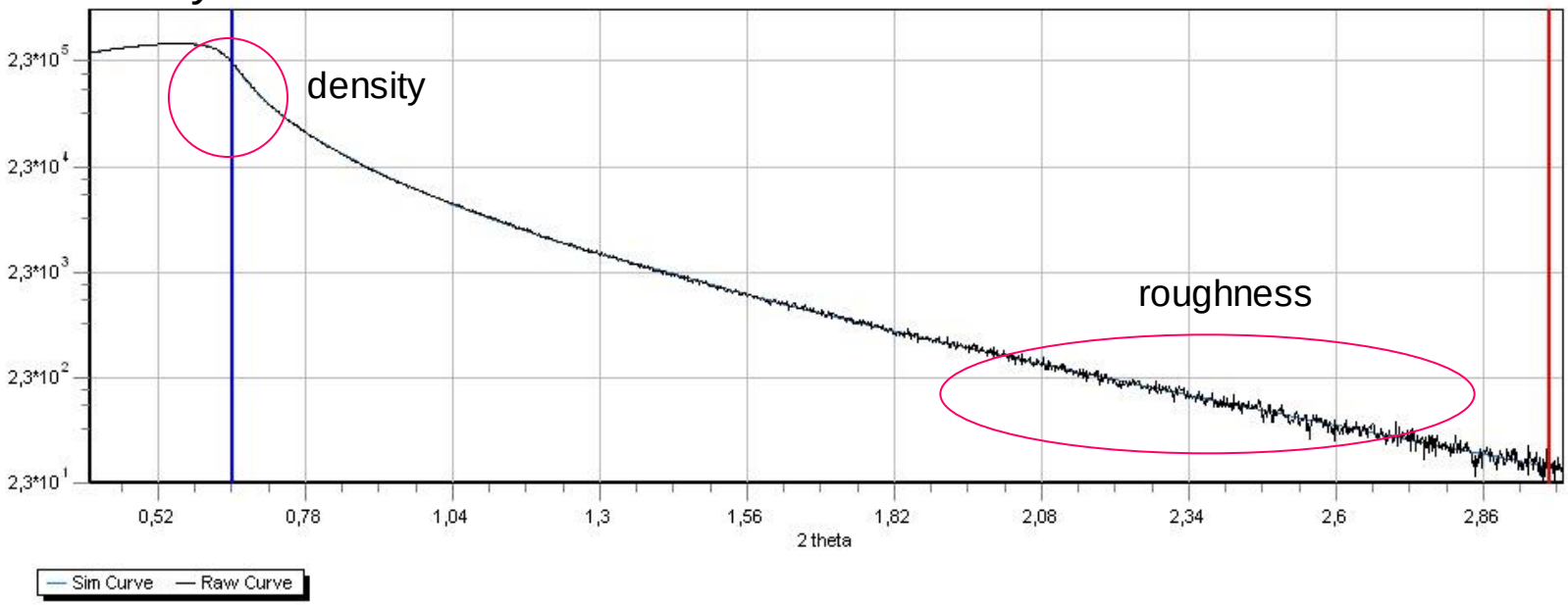

2Θ-Θ Reflectivity of LGS wafer: black line – experiment, blue line - calculation. λ=1.54 Å, $CuK_{\alpha 1}$ radiation

Structure of LGS wafer

#	Thickness, nm	Roughness, nm	Density, g/cm^3
Damaged layer 2	1.64	0.41	4.62
Damaged layer 1	2.67	0.32	5.42
Substrate	0.0	0.20	5.67

Investigation of Ir layer

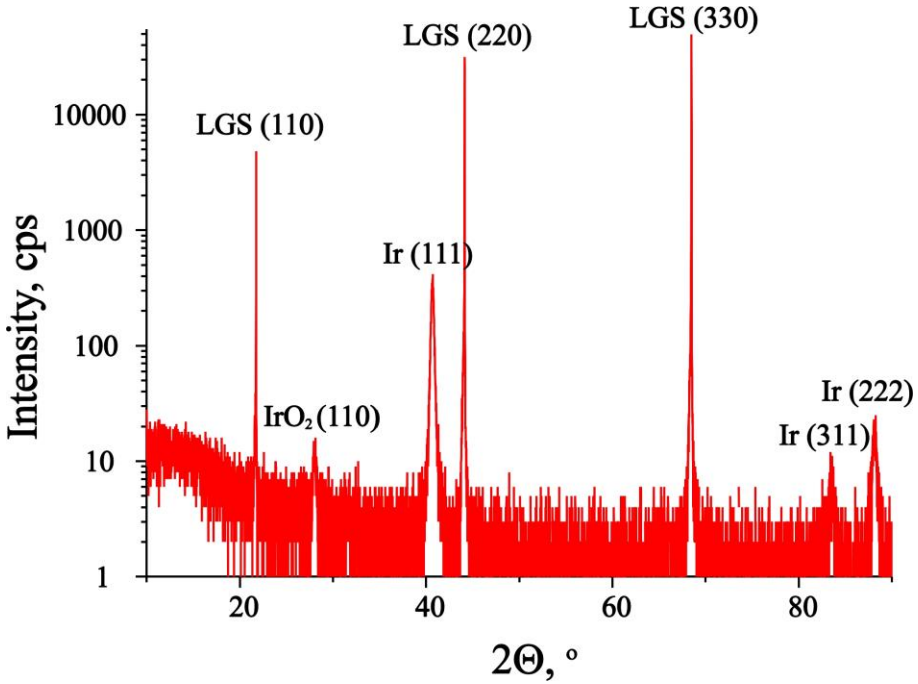

(a)

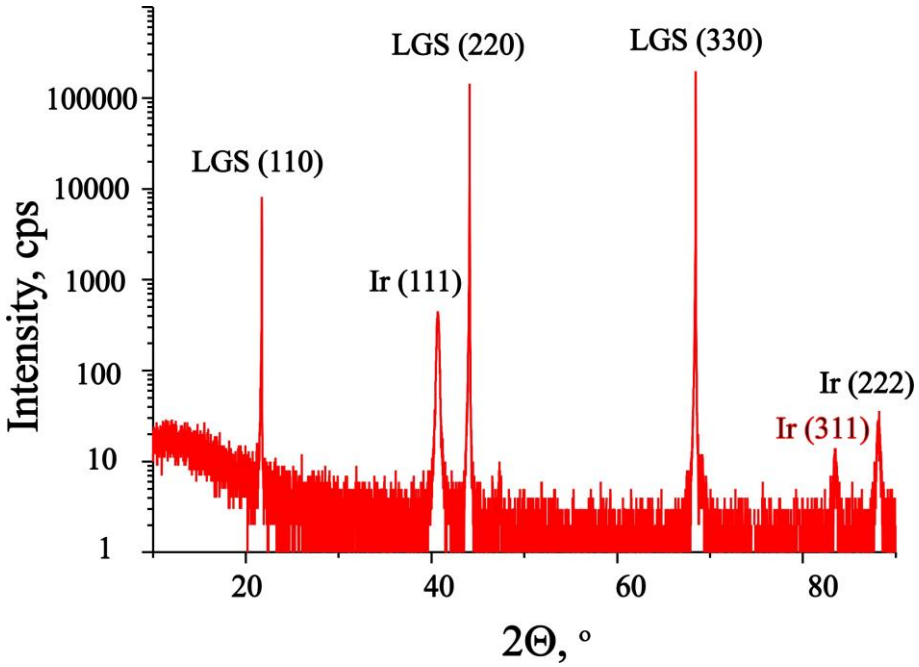

(b)

XRD diffraction spectrum of LGS crystal covered by Ir film with thickness of 1000 Å: (a) annealing in air during 400 hours at T=650°C; (b) annealing in vacuum during 20 hours at T=950°C.

λ=1.54 Å, $CuK_{\alpha 1}$ radiation

Fabrication of SAW-resonator

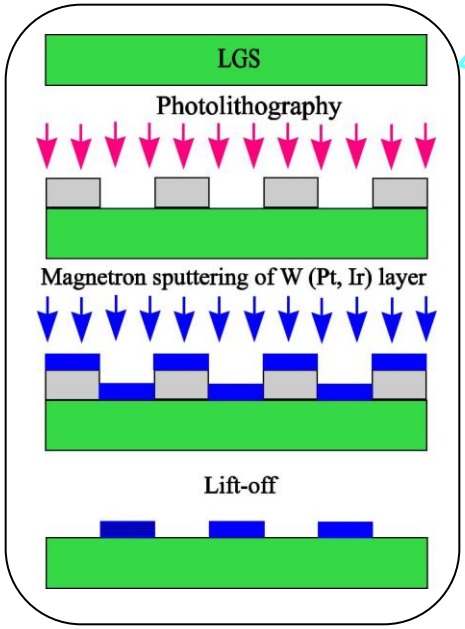

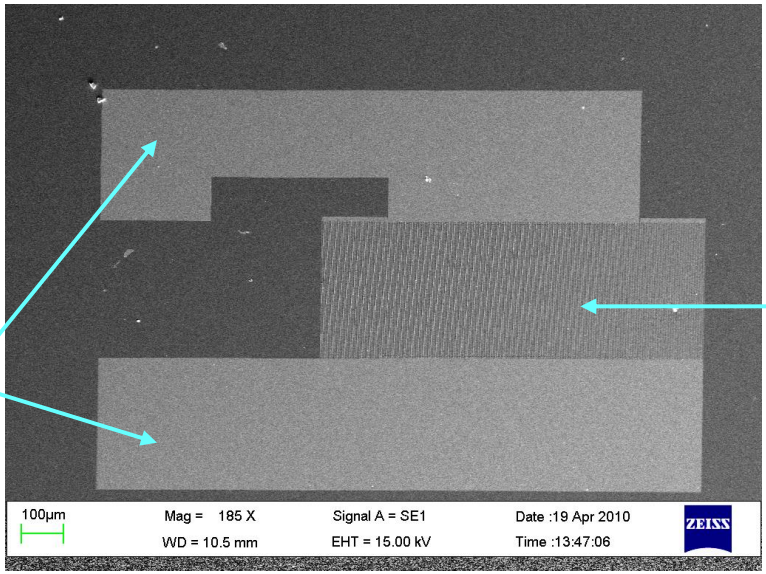

SAW-resonator structure (Λ=5.948 µm)

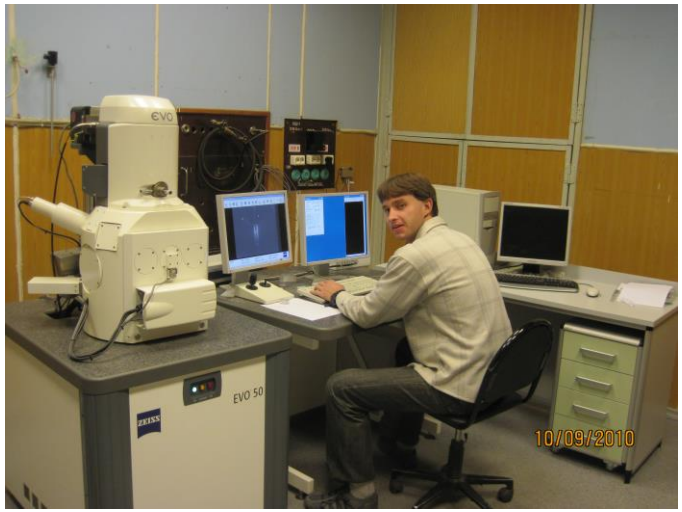

SEM ZEISS EVO-50 + NanoMaker:
E-beam lithography

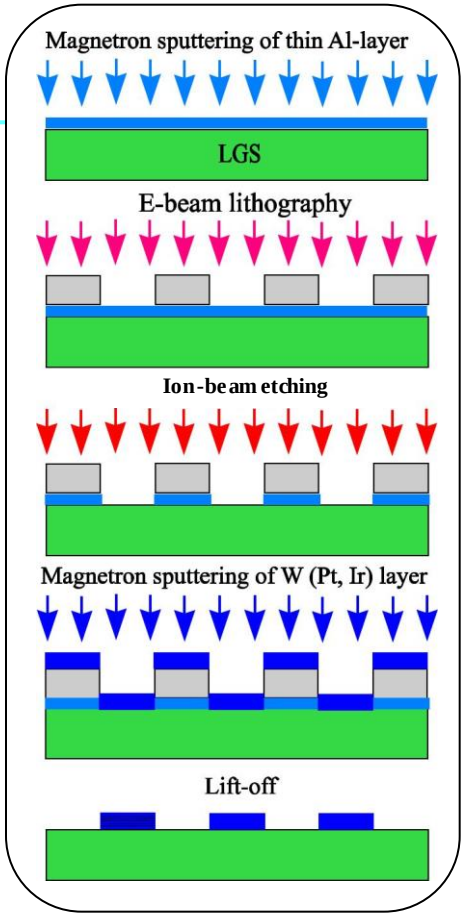

Different types of the SAW resonators (Ir)

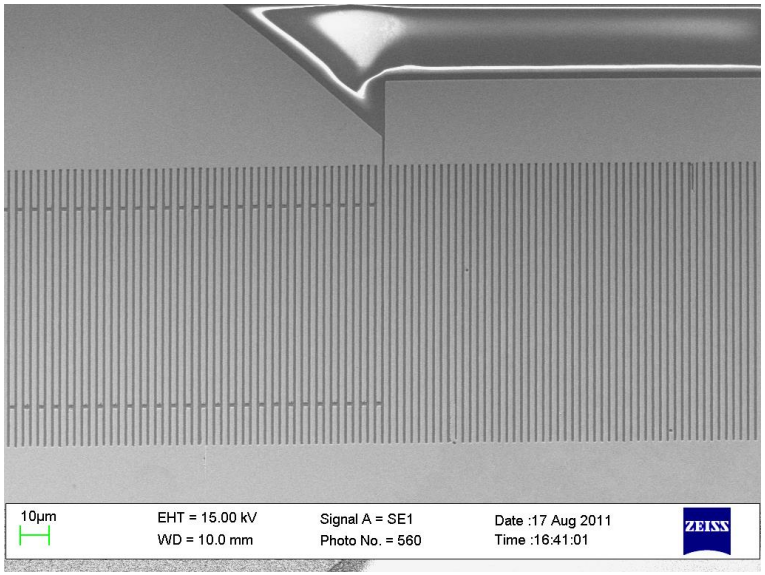

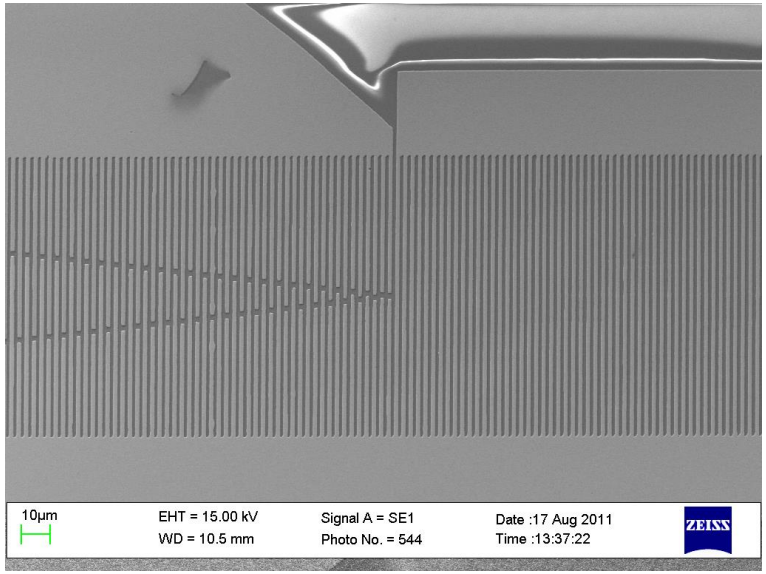

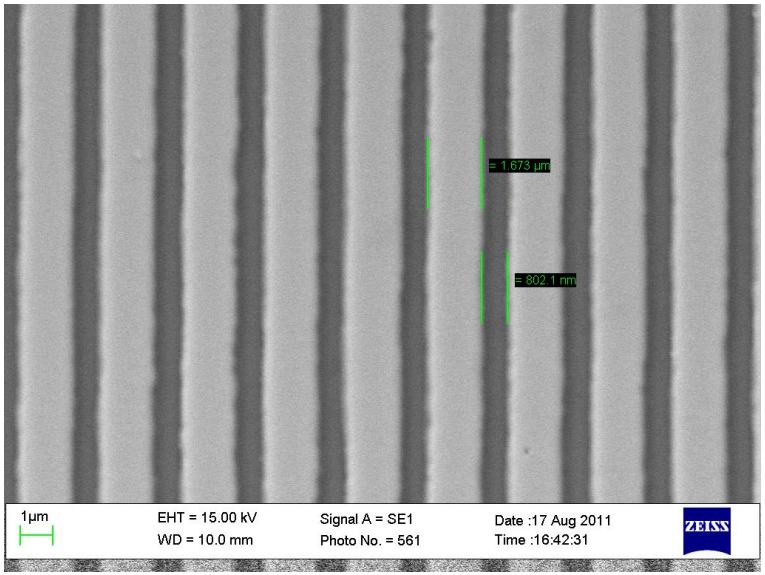

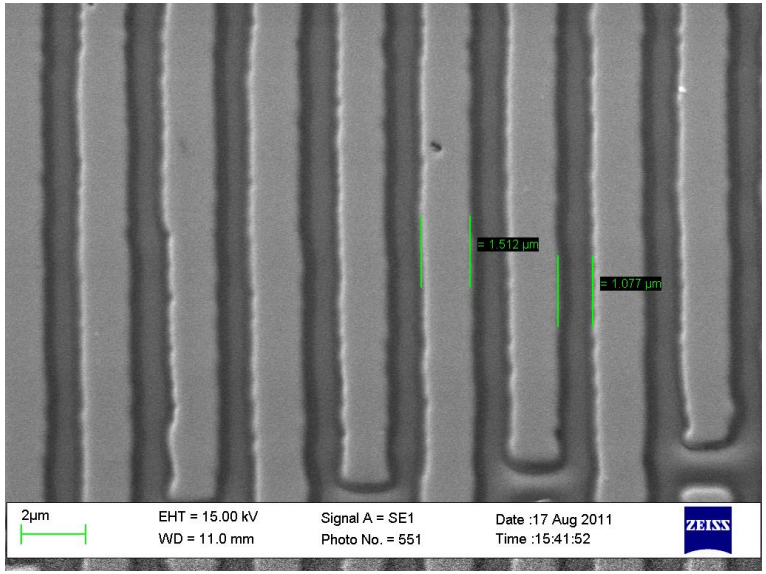

Ordinary SAW transducer

Apodized SAW transducer

Structure of *Ir* electrodes measured by AFM

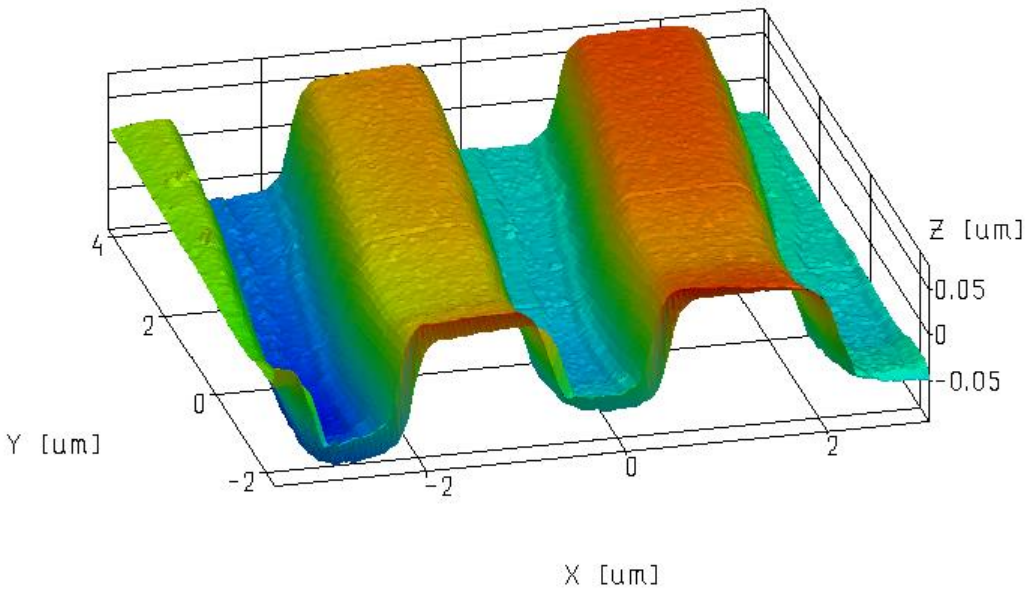

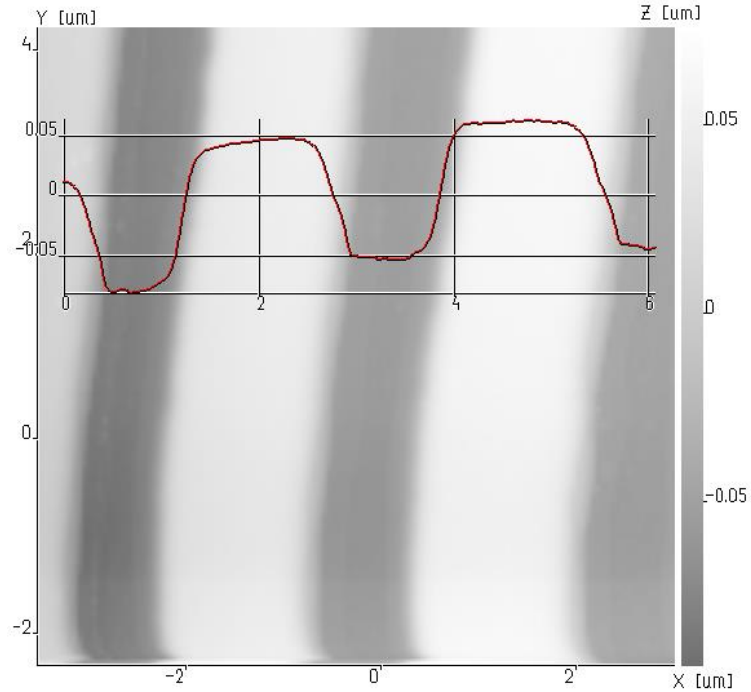

Thickness of Ir electrodes is 100 nm

SAW-resonators

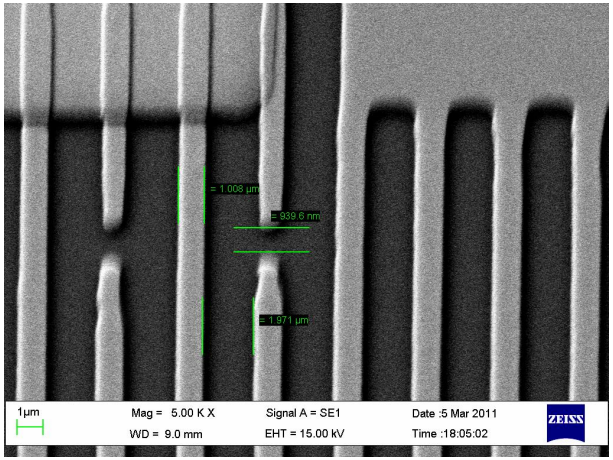

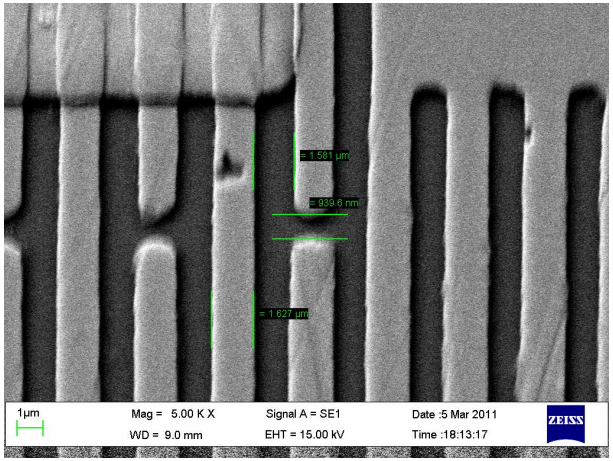

Coefficient of metallization 34%
f=409 MHz, V=2432.732 m/s

Coefficient of metallization 51%
f=402 MHz, V=2391.096 m/s

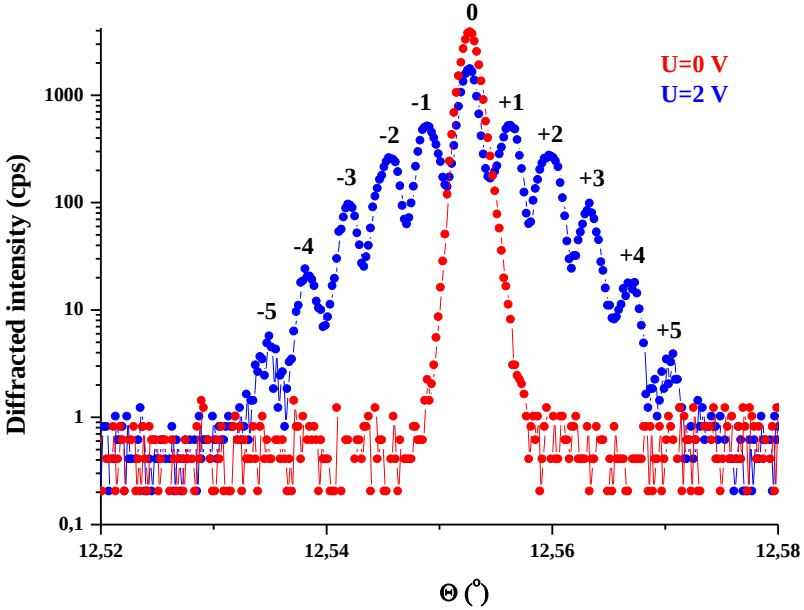

Rocking curve

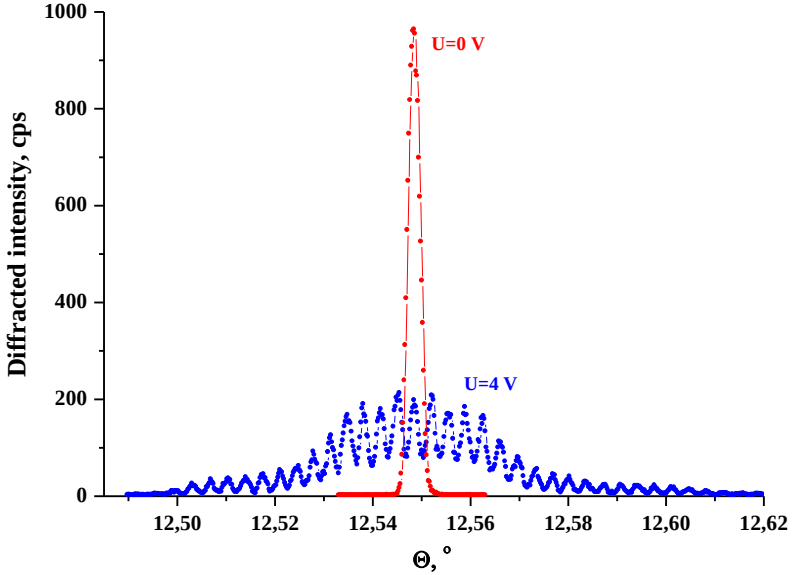

Rocking curve

6. Fast X-Ray beam chopper

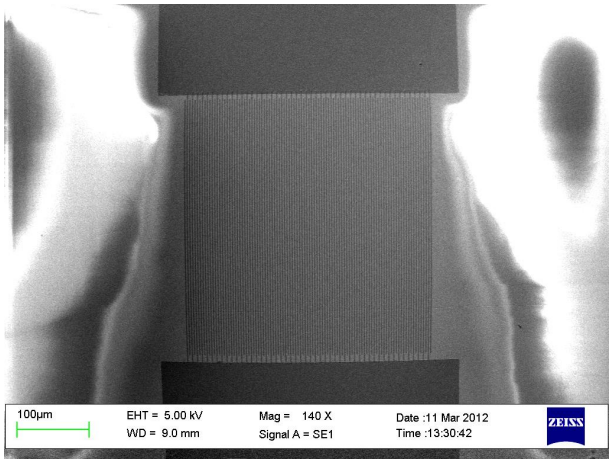

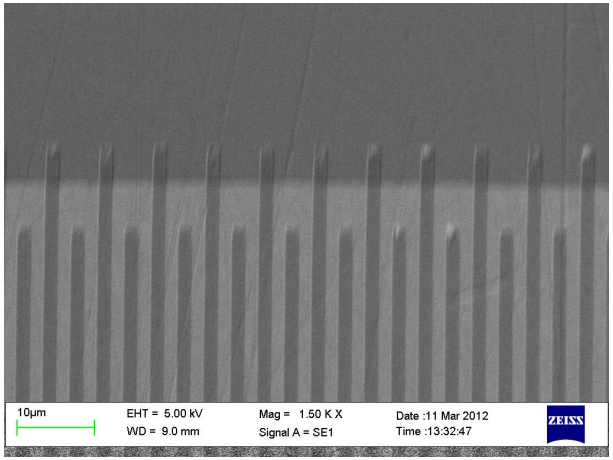

Λ=4 µm, W=60×Λ=240 µm

SAW delay time line based on the *X*-cut of CTGS crystal: Λ=4 µm, f=700 MHz

X-ray diffraction by *X*-cut of CTGS crystal modulated by SAW with wavelength of Λ=4 μm. Reflection (110), Θ_B=11.008º, f_0=700 MHz, *V*=2800 m/s, surface roughness 4.1 Å

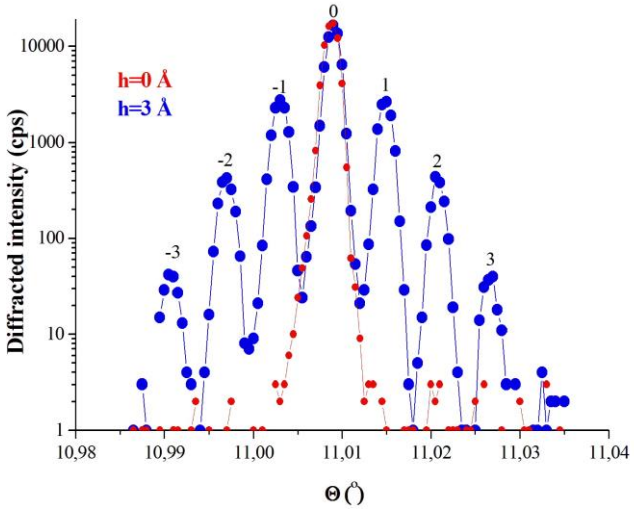

Rocking curve, *U*=2 V

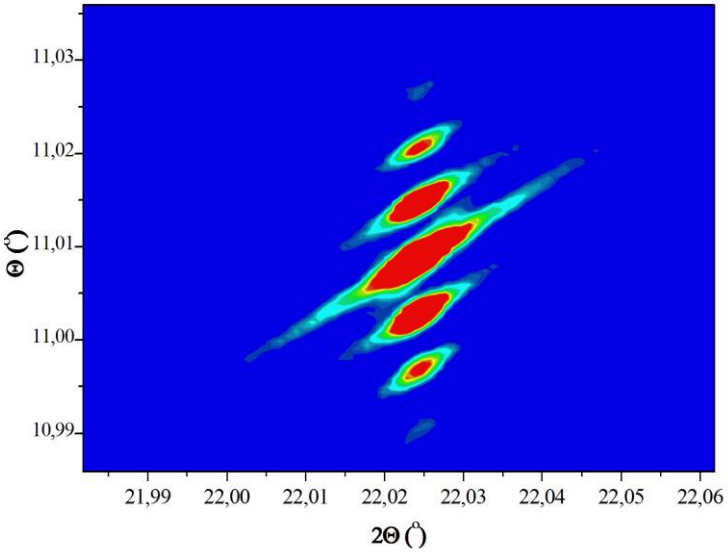

2D map of the diffracted X-ray intensity

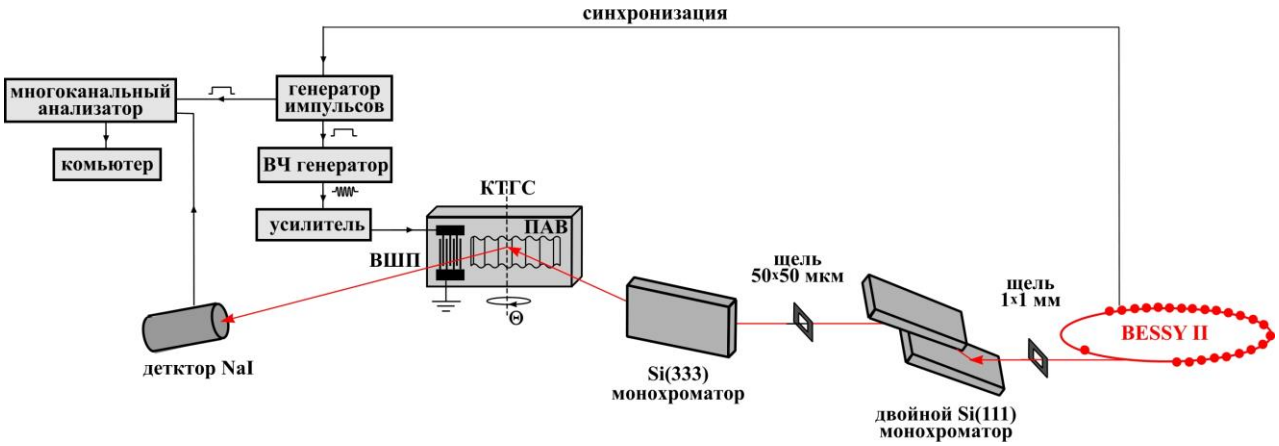

Experimental set-up of a high-frequency X-ray beam chopper

HF acoustooptic modulation of synchrotron radiation at BESSY II

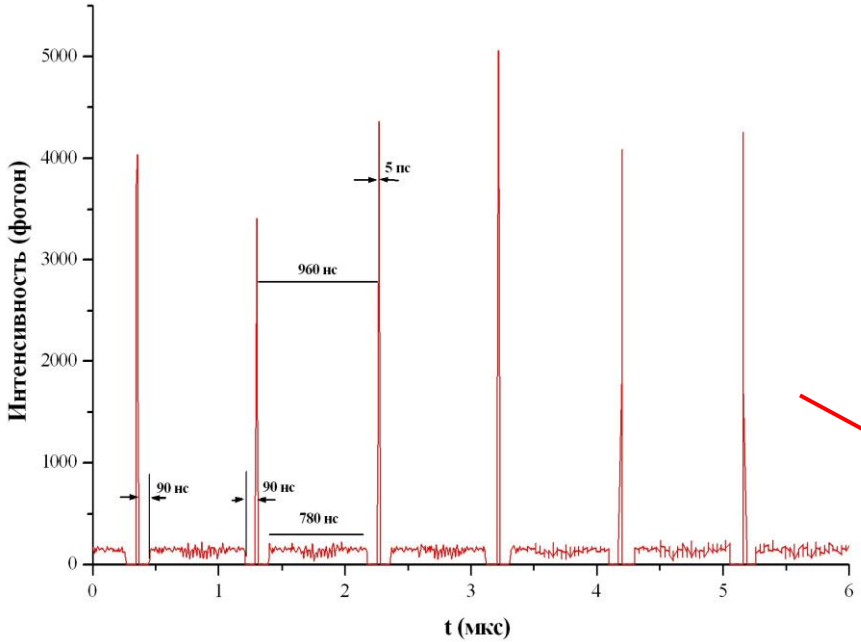

BESSY II: hybrid mode

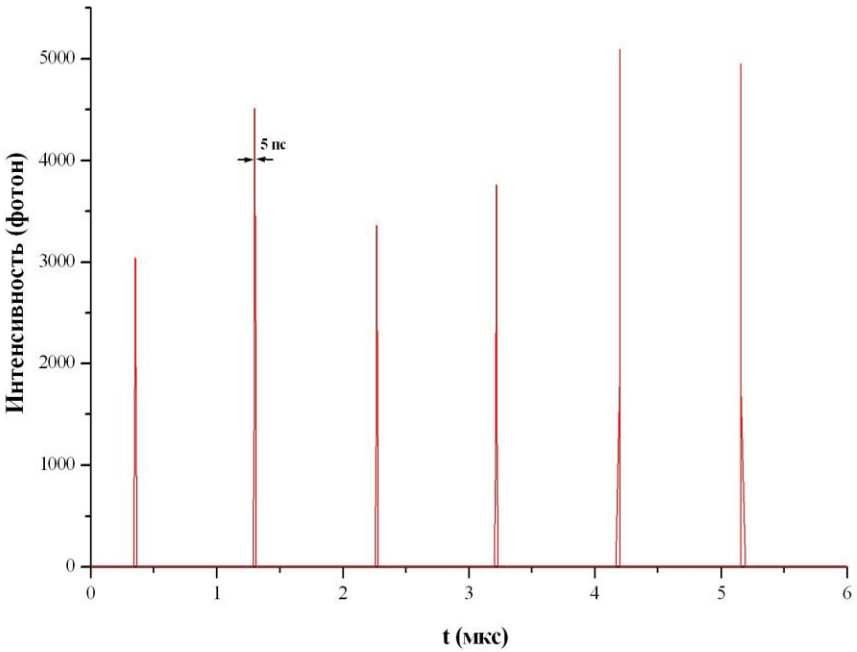

BESSY II: single bunch mode

7. SAW imaging by Talbot effect at the synchrotron radiation source

Talbot effect $Z_T=2\Lambda^2/\lambda$

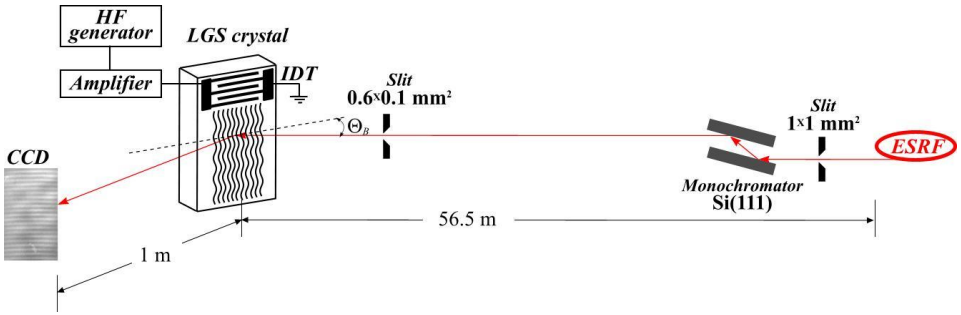

Scheme of a double crystal diffractometer. Saggital diffraction geometry.

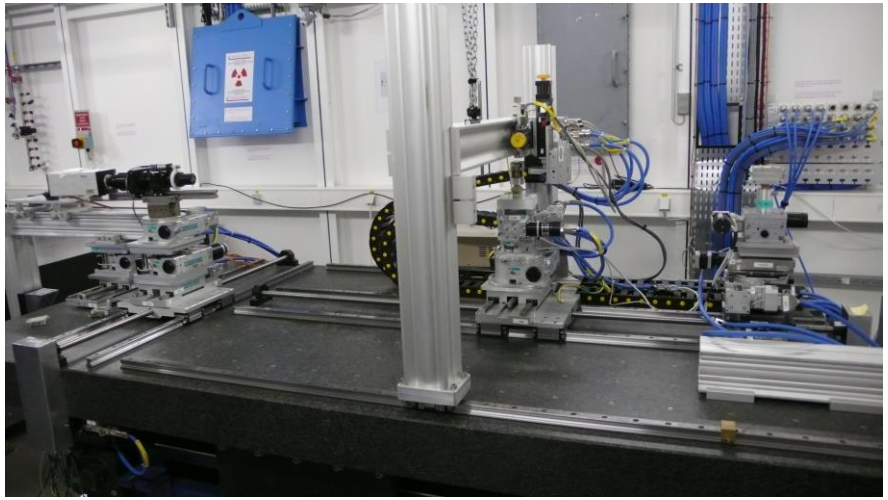

Optical beamline ID06, ESRF

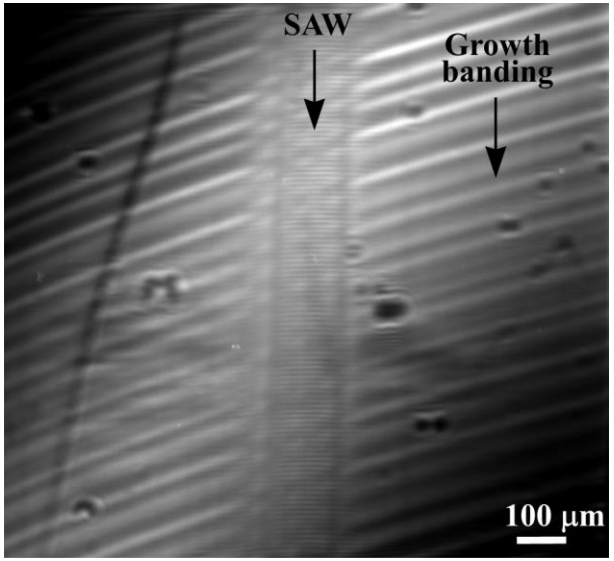

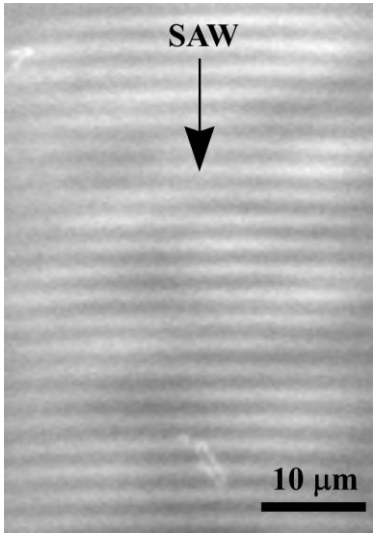

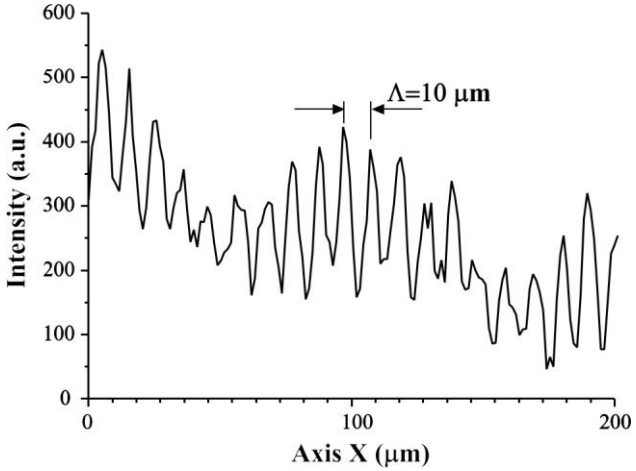

Acoustically modulated *Y*-cut of an LGS crystal.
Reflection (100), Λ=10 μm, λ=1Å.

SAW imaging at BESSY II, optical beamline KMC 2

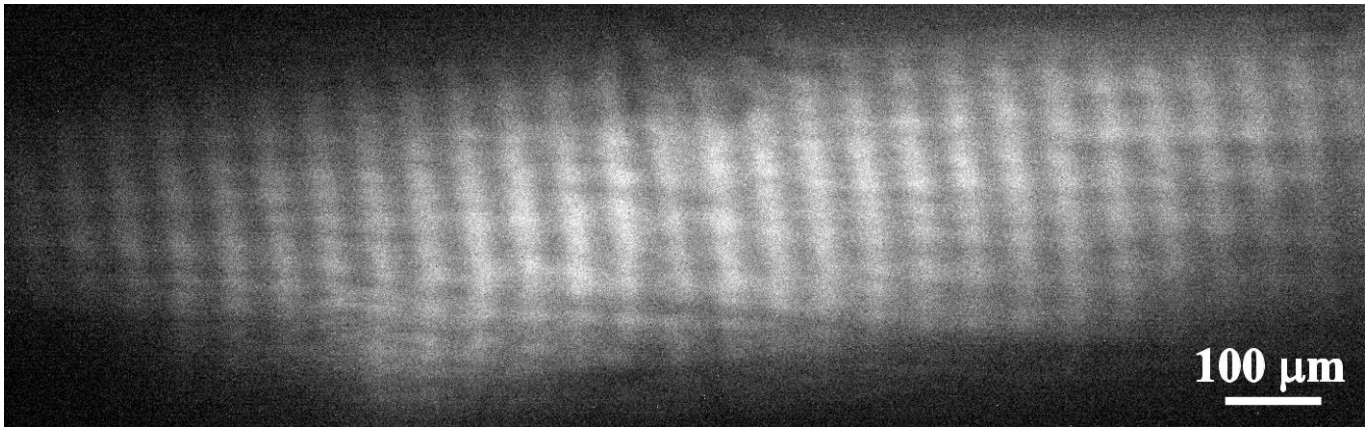

Y-cut of a CTGS crystal, Λ=50 µm, f=46.373 MHz

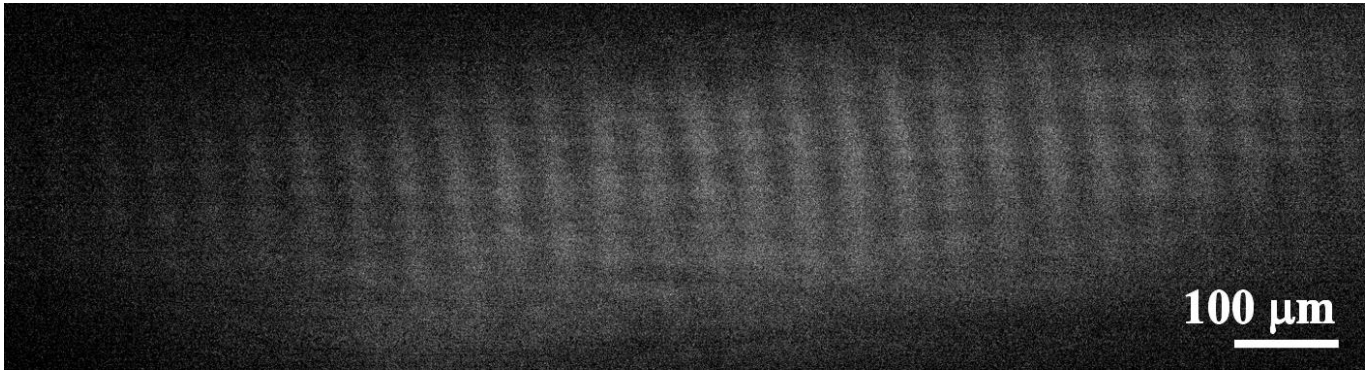

Y-cut of a CTGS crystal, Λ=50 µm, f=46.563 MHz

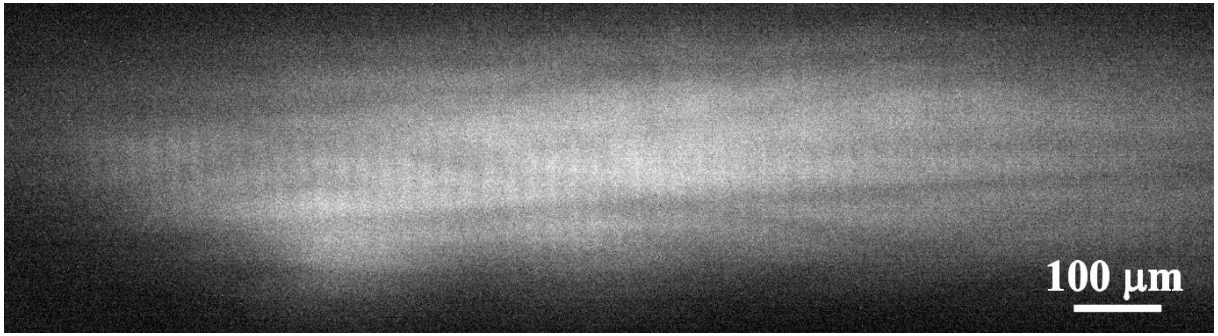

Y-cut of a CTGS crystal, Λ=28 μm, f=100.4186 MHz

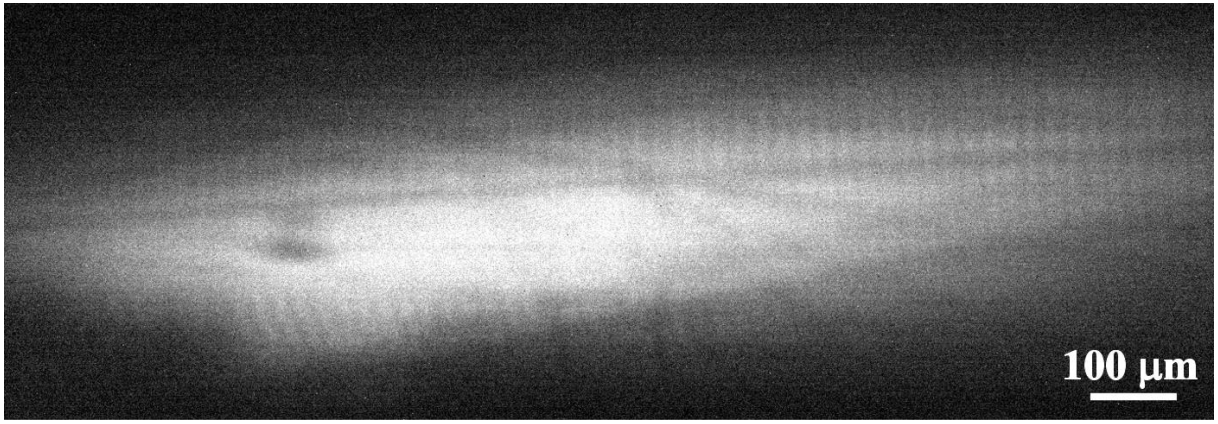

Y-cut of a CTGS crystal, Λ=28 μm, f=100.4565 MHz

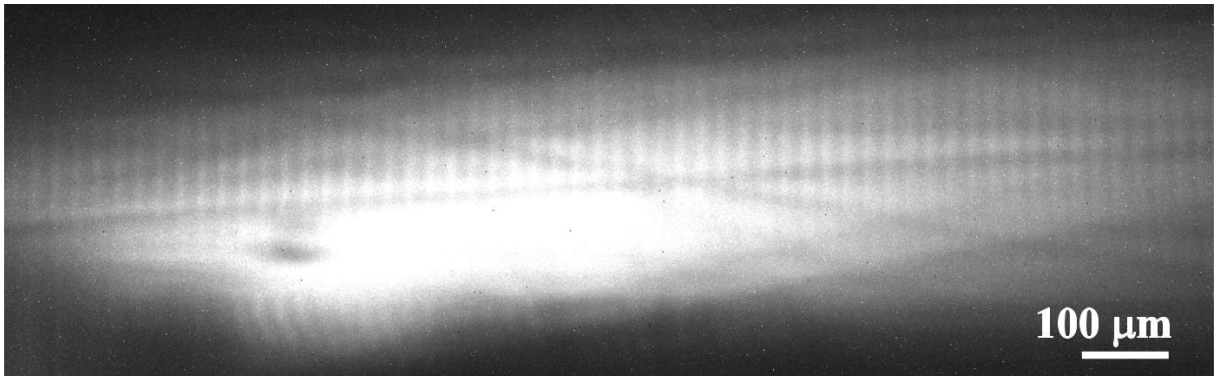

Y-cut of a CTGS crystal, Λ=28 μm, f=100.4734 MHz

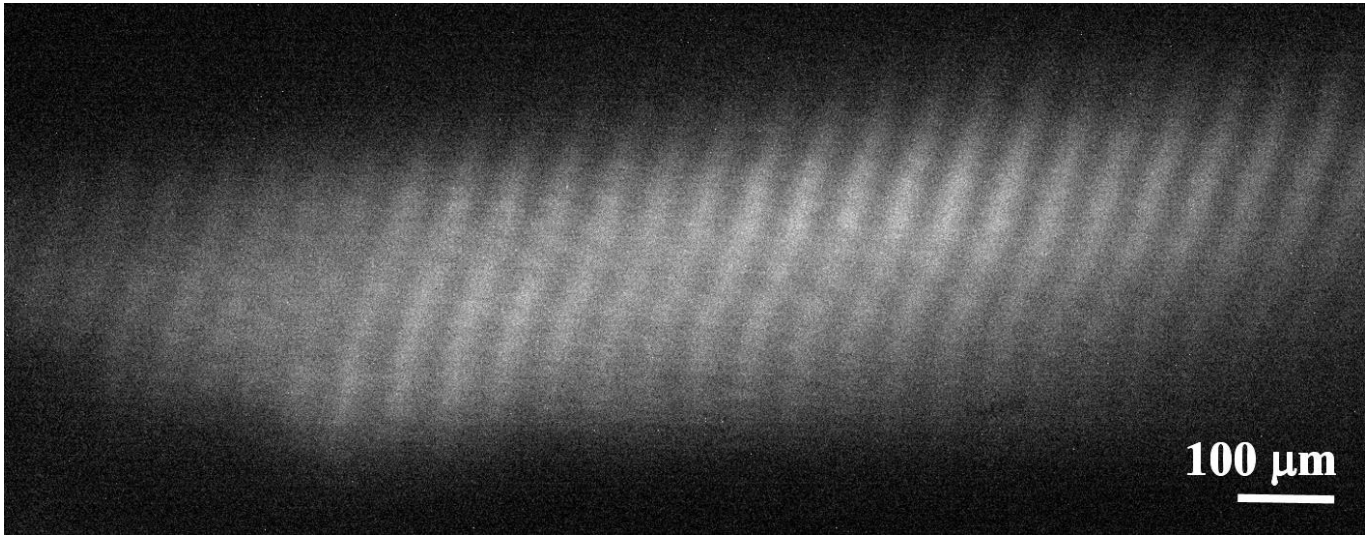

Y-cut of an LGS crystal, Λ=50 μm, f=39.387 MHz

8. Ordering $Ca_3TaGa_3Si_2O_{14}$ crystal

X-ray diffraction by *X*-cut of a CTGS crystal modulated by SAW with wavelength of Λ=4 μm. E=11 keV, λ=1.166 Å, reflection (110), Θ_B=7.7764º, f_0=700 MHz, *V*=2800 m/s

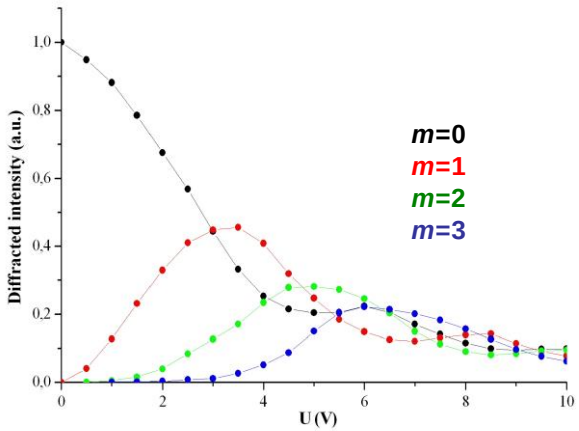

Diffracted intensity versus amplitude

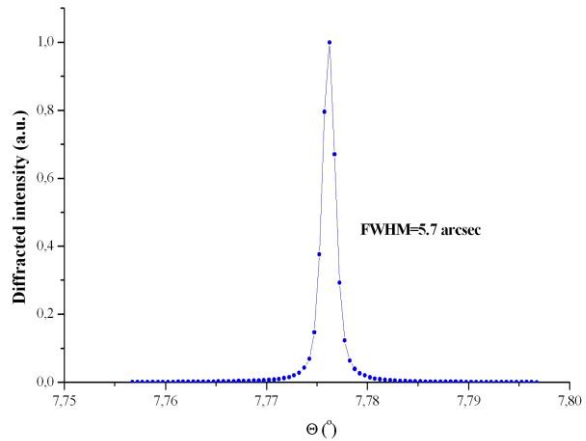

U=0 V

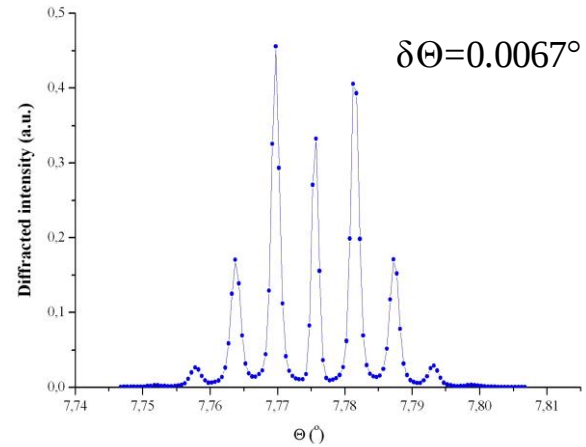

U=3.5 V

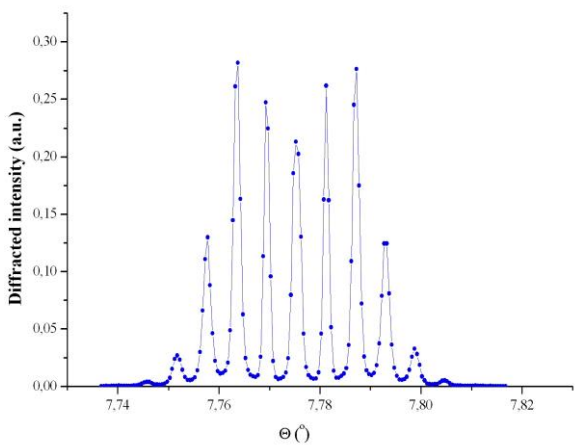

U=5 V

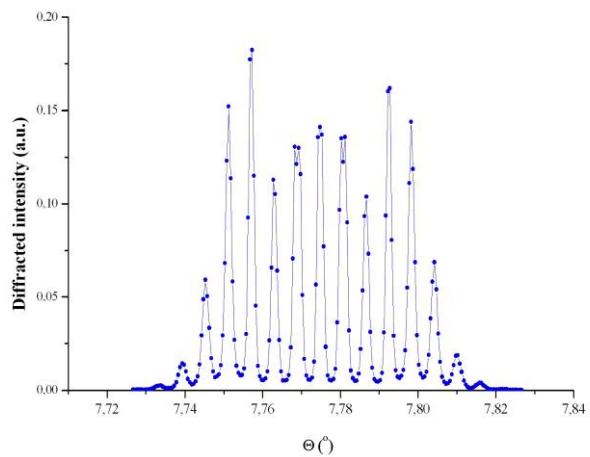

U=7.5 V

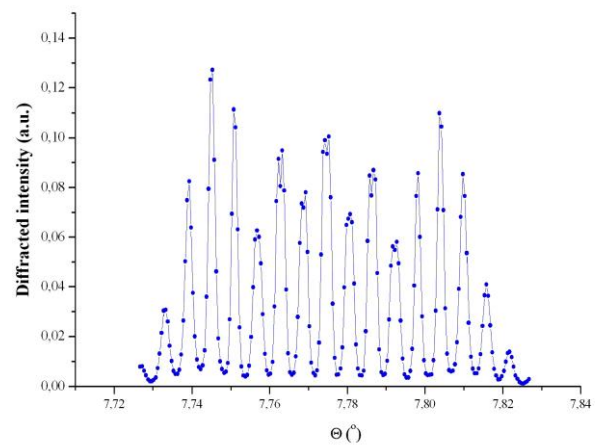

U=10 V

X-ray diffraction by *X*-cut of a CTGS crystal modulated by SAW with wavelength of Λ=4 μm. E=11 keV, λ=1.166 Å, reflection (110), Θ_B=7.7764º, f_0=700 MHz, *V*=2800 m/s

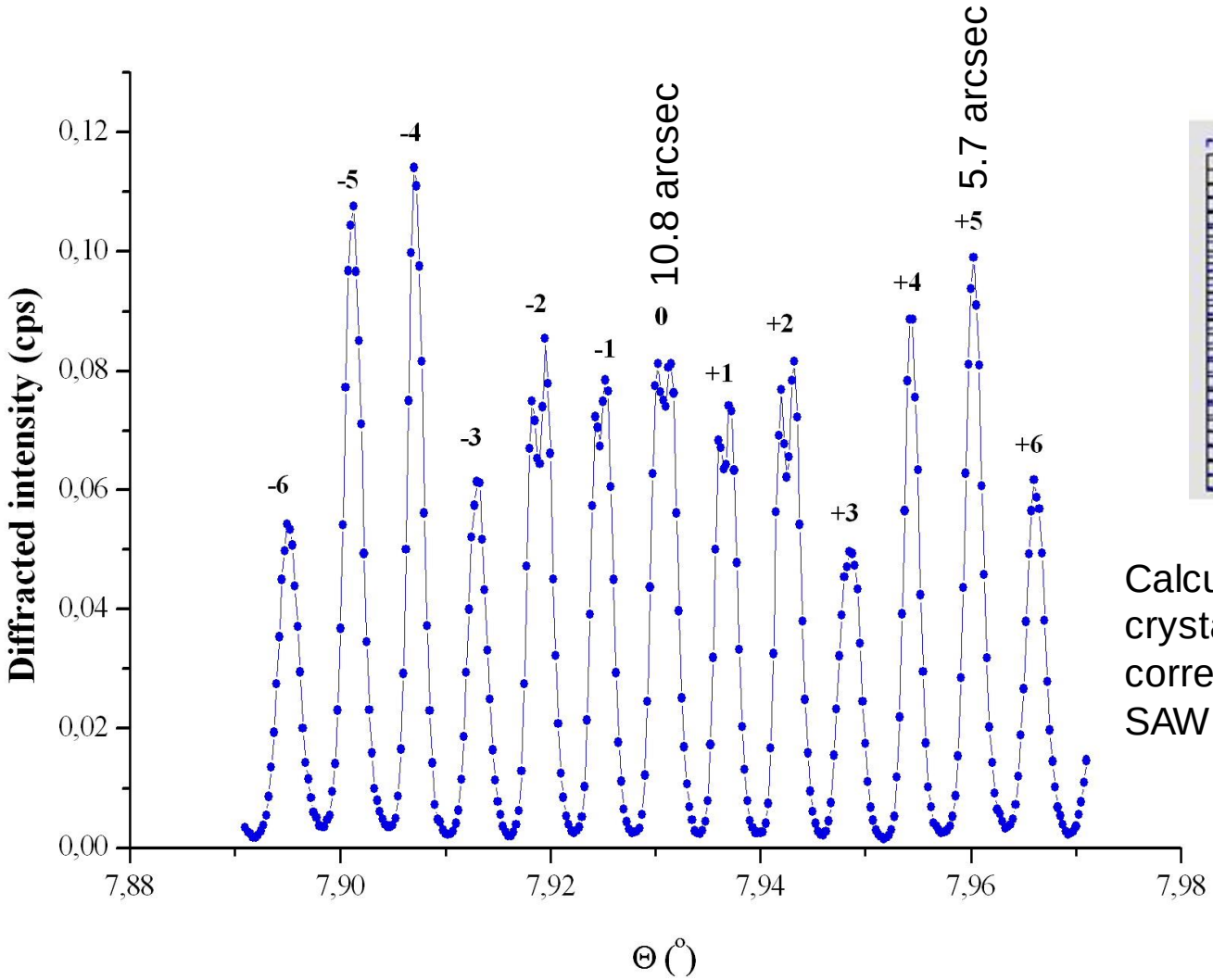

Rocking curve, *U*=10 V

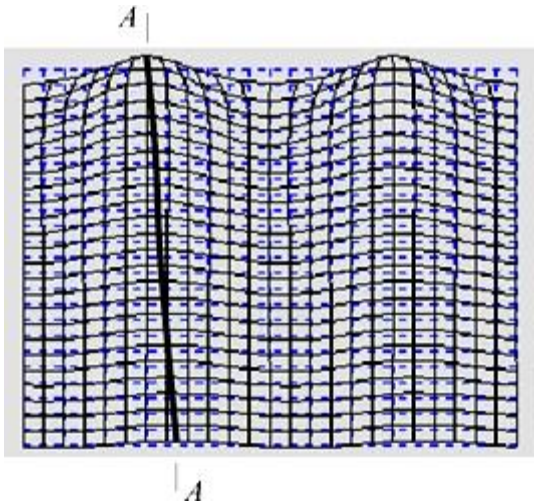

Calculated deformation of a crystal lattice by SAW. Line (AA) corresponds to the position of the SAW maxima inside the crystal.

Y-cut of CTGS crystal

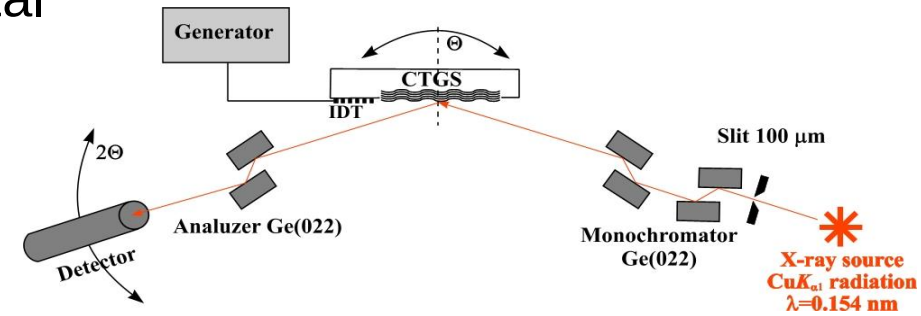

Experimental set-up of a triple-axis X-ray diffractometer

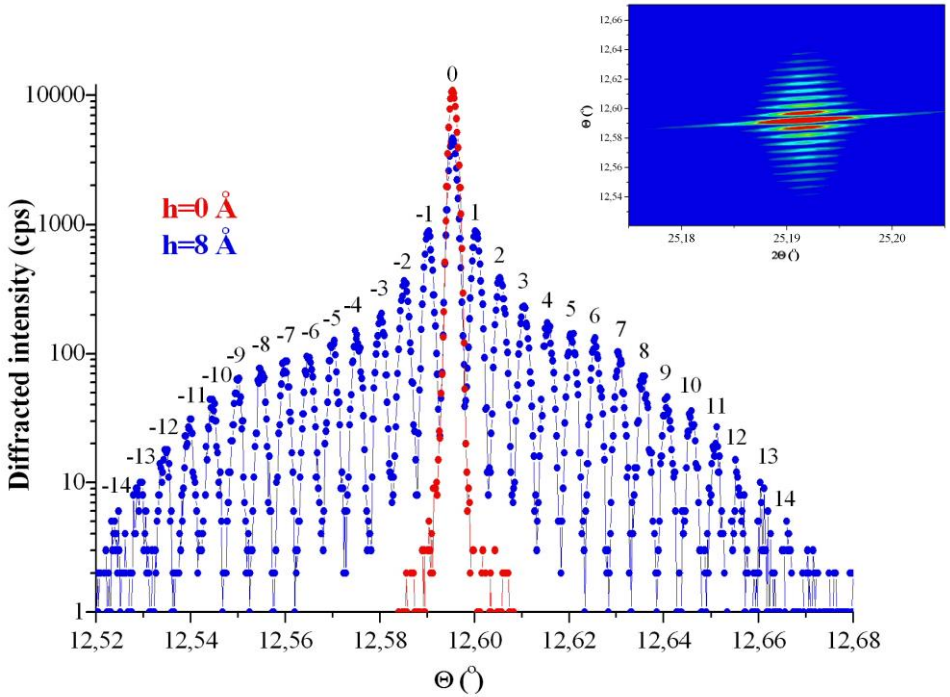

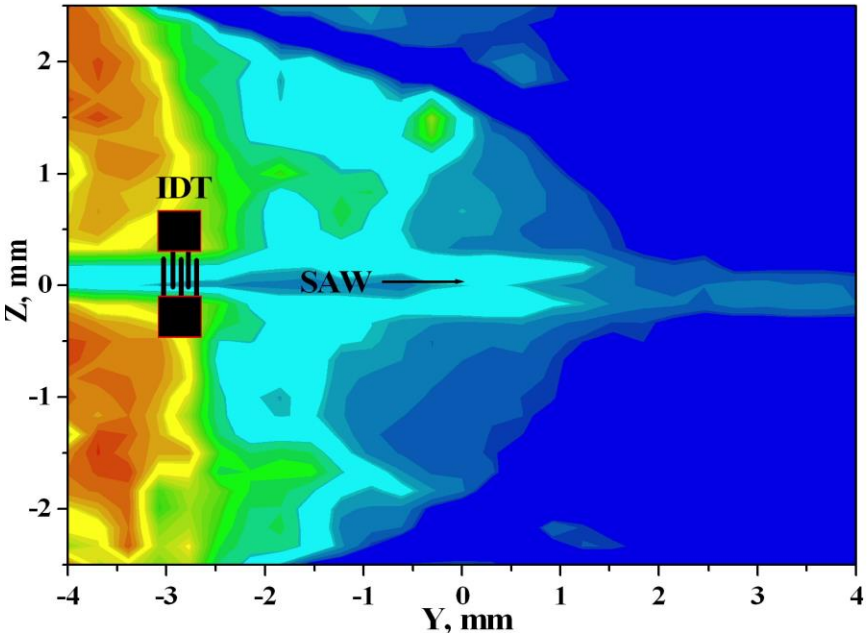

X-ray diffraction by the *Y*-cut of a CTGS crystal modulated by a SAW: rocking curves measured at SAW amplitudes h_0=0 Å and h_0=8 Å; 2D map of the distribution of the diffracted X-ray radiation on the crystal surface. λ=1.54 Å; (200) reflection; Θ_B=12.598°; f_0=693 MHz; V=2772 m/s; Λ=4 μm.

X-cut of CTGS crystal

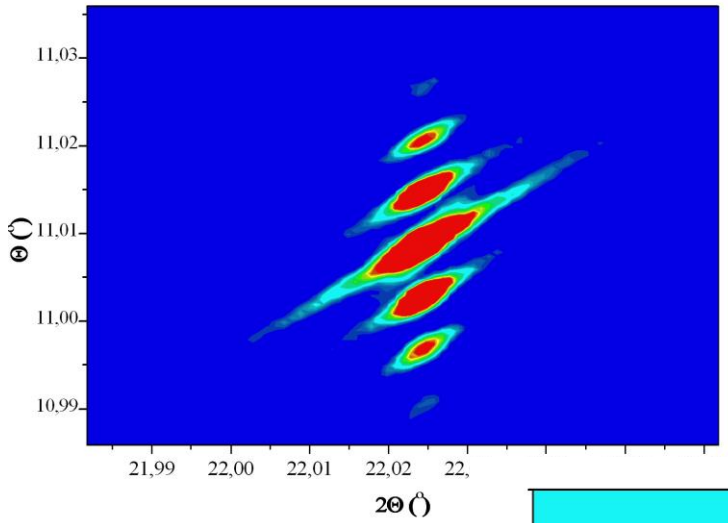

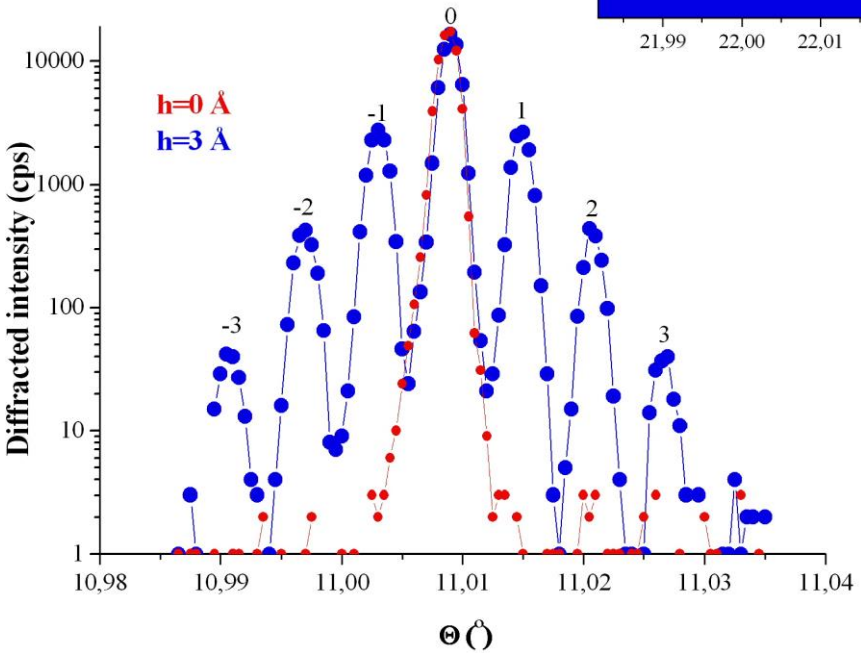

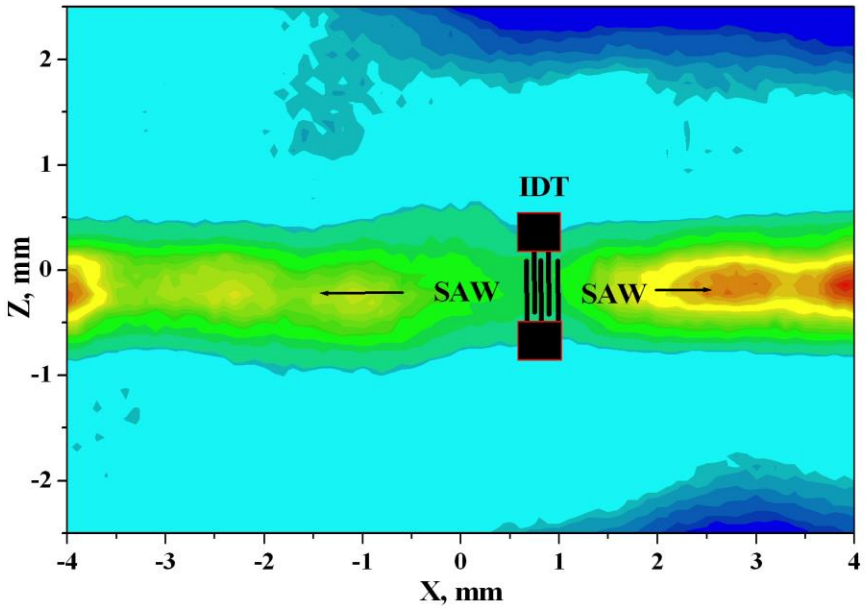

X-ray diffraction by the *X*-cut of a CTGS crystal modulated by a SAW: rocking curves measured at SAW amplitudes h_0=0 Å and h_0=3 Å; 2D map of the distribution of the diffracted X-ray radiation on the crystal surface. λ=1.54 Å; (200) reflection; Θ_B=12.598º; f_0=700 MHz; V=2800 m/s; Λ=4 μm.

9. Non-ordering $La_3Ga_{5.3}Ta_{0.5}Al_{0.2}O_{14}$ crystal

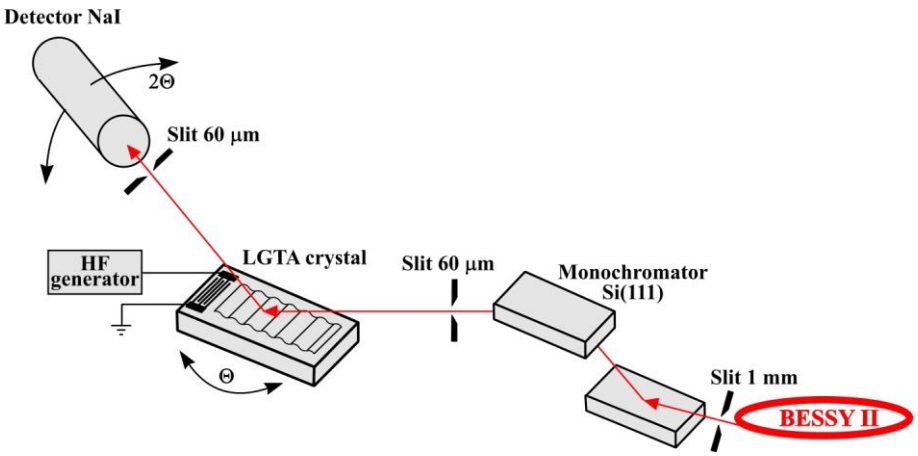

Experimental setup of a double axis X-ray diffractometer at BESSY II

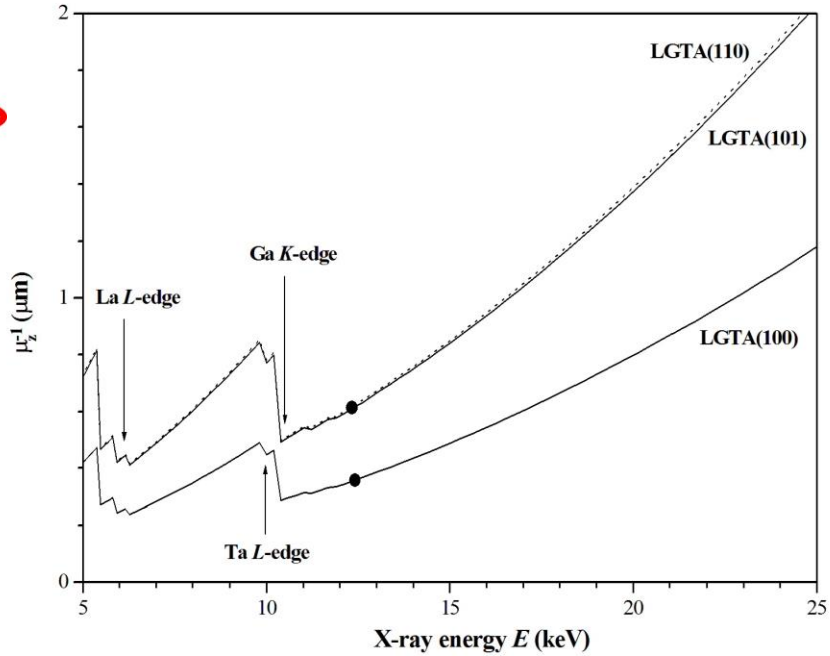

X-ray penetration depth in LGTA crystal for (100), (110), and (101) reflections versus X-ray energy. Black circles show the energy of *E*=12.5 keV.

Y-cut of LGTA crystal: reflection(100); Θ_B=3.990°; Λ=6 μm; *f*=370 MHz; *V*=2220 m/s.

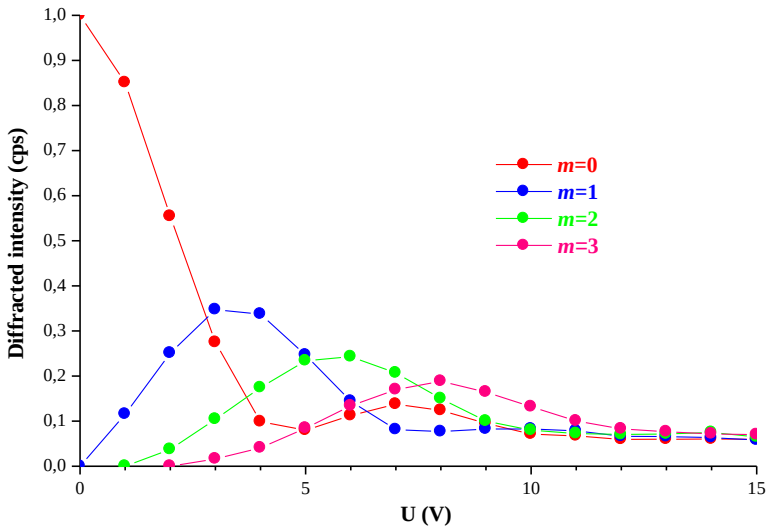

Intensities of the diffraction satellites vs. amplitude of the input signal supplied to the IDT.

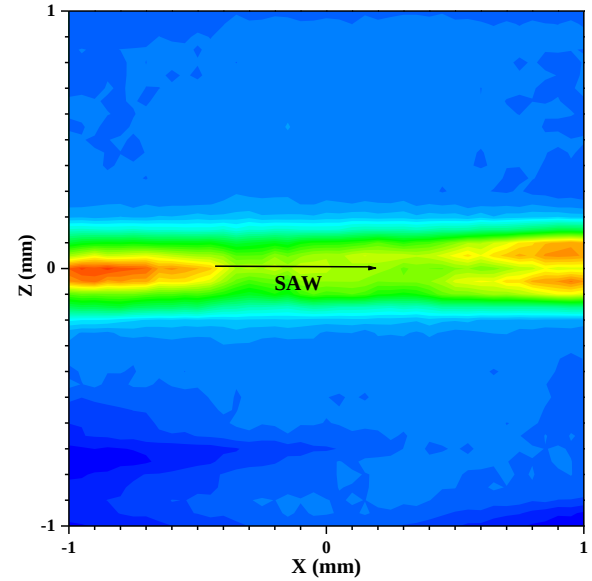

Map of the diffracted X-ray intensity at the *Y*-cut of an LGTA modulated by SAW. *α*=0.0°.

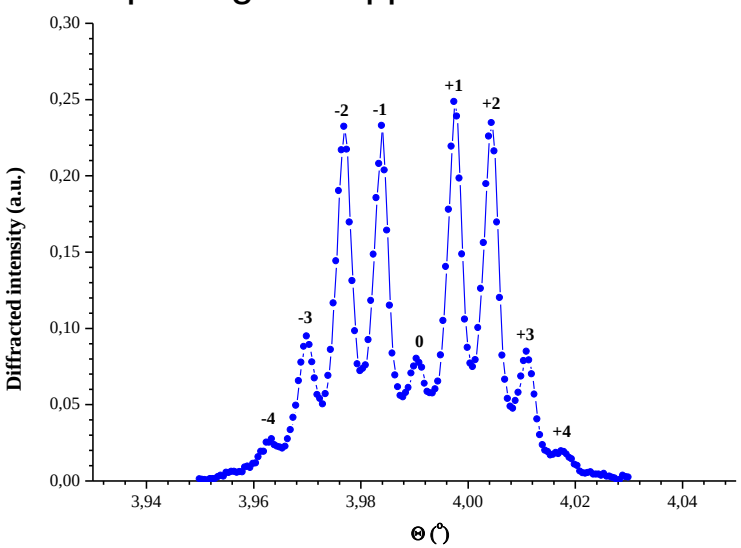

U=5 V

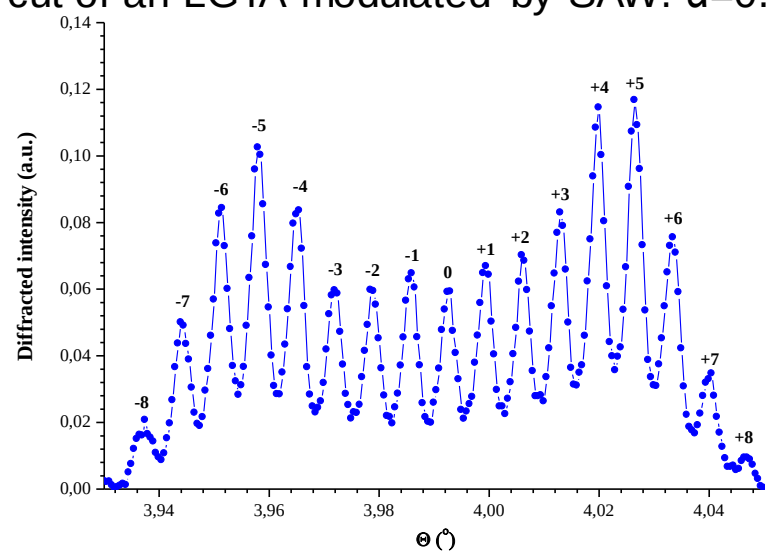

U=12 V

Rocking curves measured for different amplitudes of the input signal supplied to the IDT.

X-cut of LGTA crystal: reflection (110); Θ_B=7.030°; Λ=6 μm; *f*=390 MHz; *V*=2340 m/s.

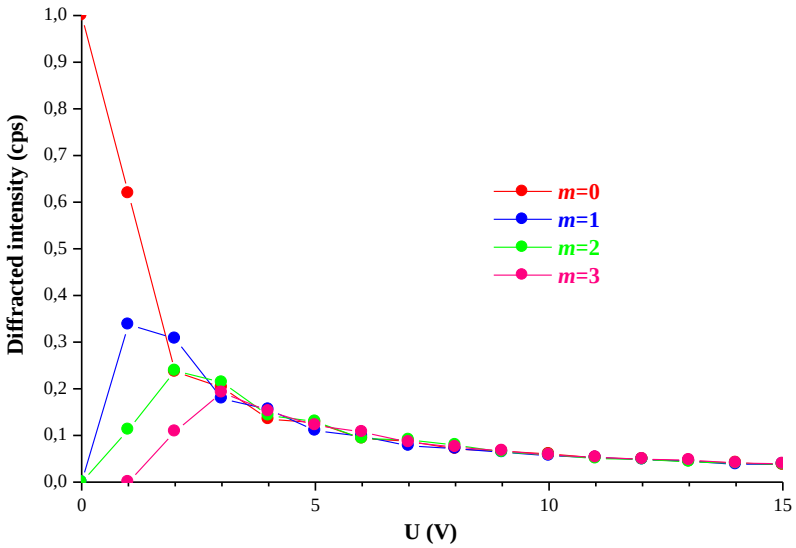

Intensities of the diffraction satellites vs. amplitude of the input signal supplied to the IDT.

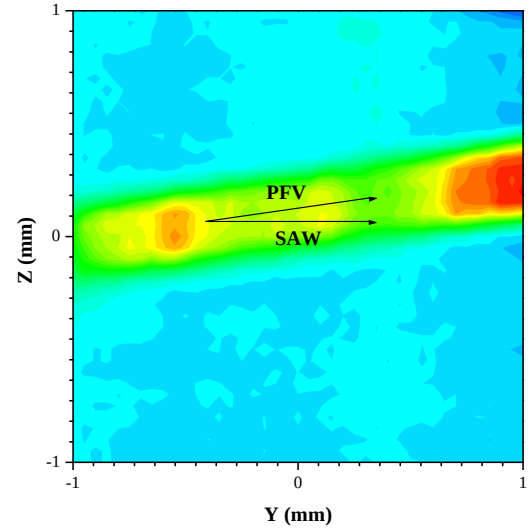

Map of the diffracted X-ray intensity at the *Y*-cut of an LGTA modulated by SAW. *α*=6.3°.

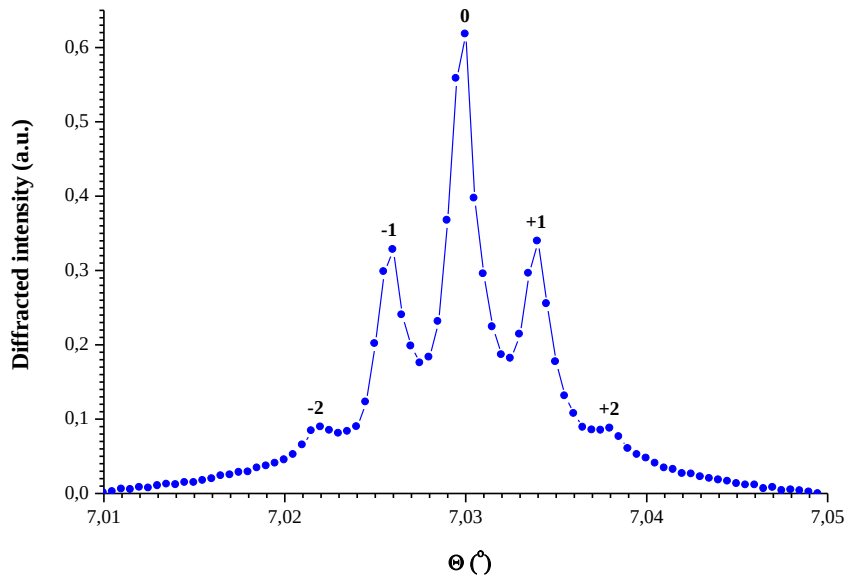

U=1 V

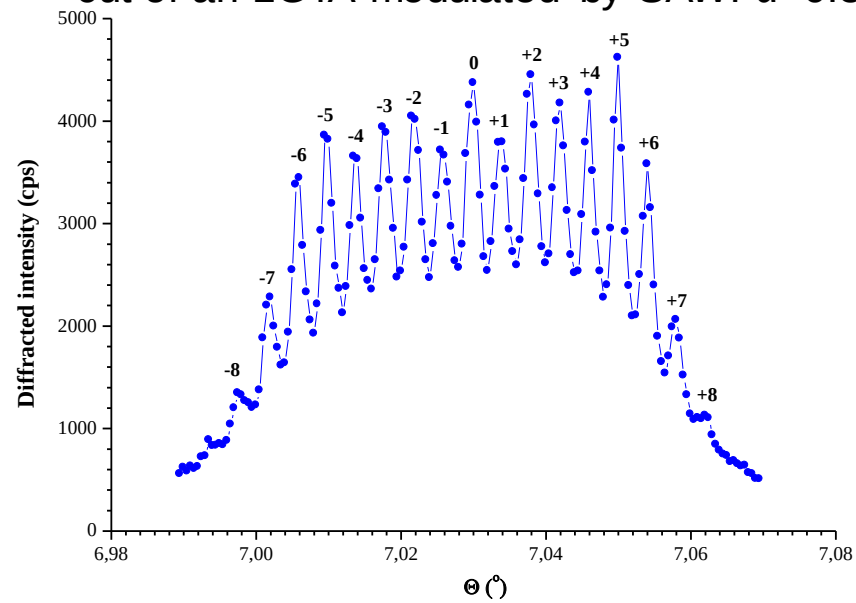

U=5 V

Rocking curves measured for different amplitudes of the input signal supplied to the IDT.

yxl/+36°-cut of LGTA crystal: reflection (101); Θ_B=6.996°; Λ=6 μm; *f*=437 MHz; *V*=2622 m/s.

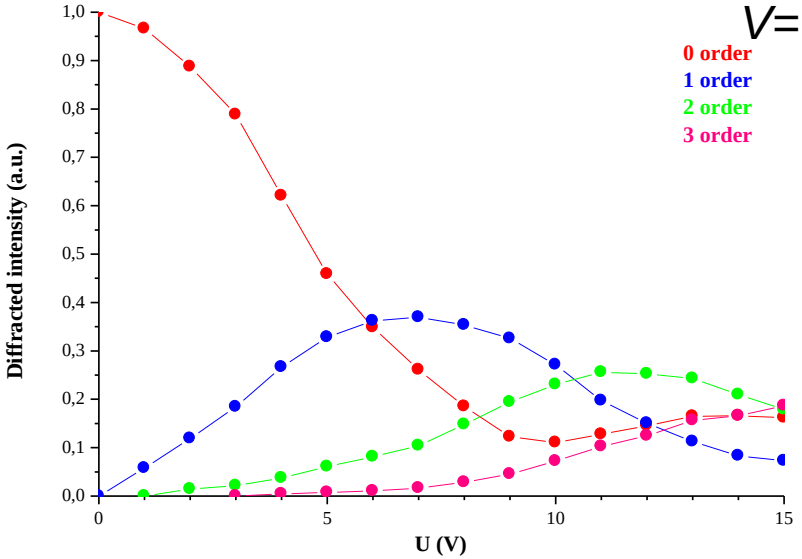

Intensities of the diffraction satellites vs. amplitude of the input signal supplied to the IDT.

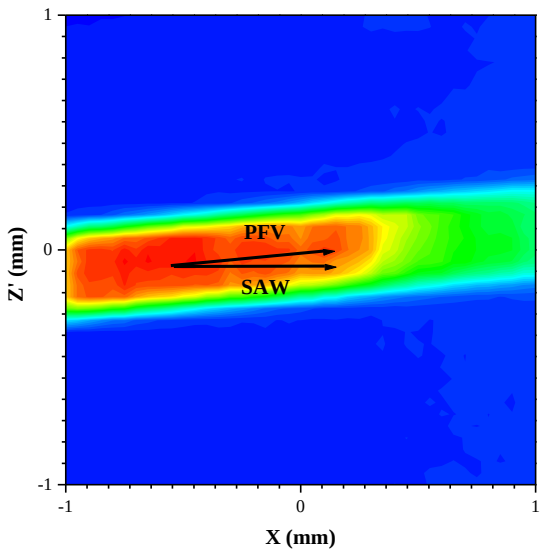

Map of the diffracted X-ray intensity at the *Y*-cut of an LGTA modulated by SAW. *α*=4.0°.

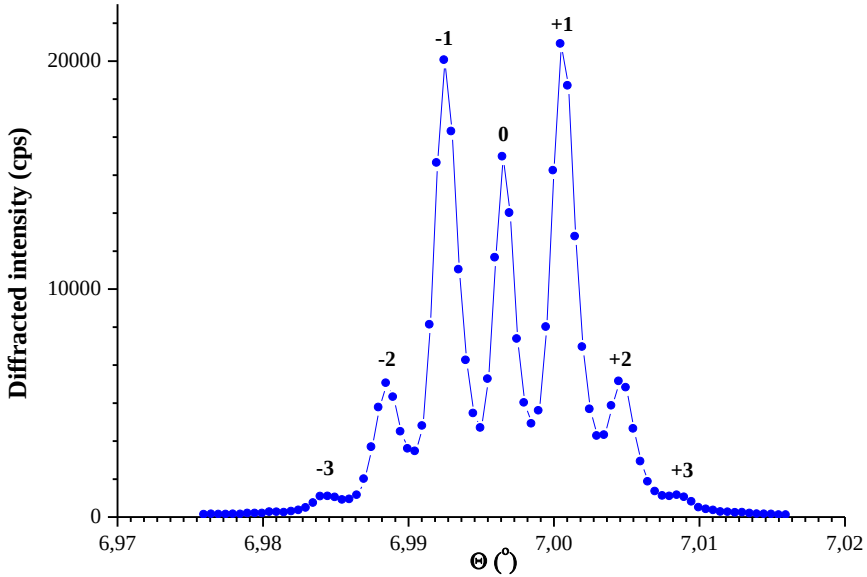

U=7 V

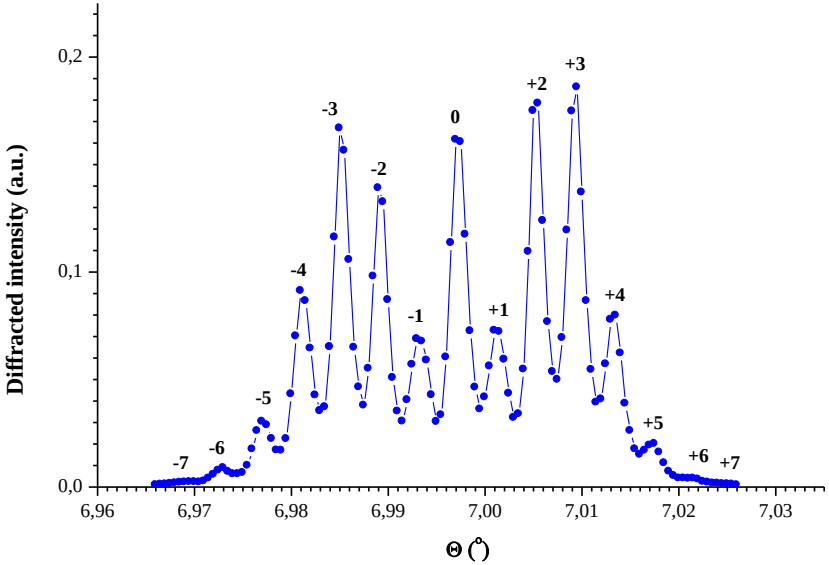

U=15 V

Rocking curves measured for different amplitudes of the input signal supplied to the IDT.

10. Investigation of surface and pseudo-surface acoustic waves excitation and propagation in $La_3Ga_5SiO_{14}$ crystal

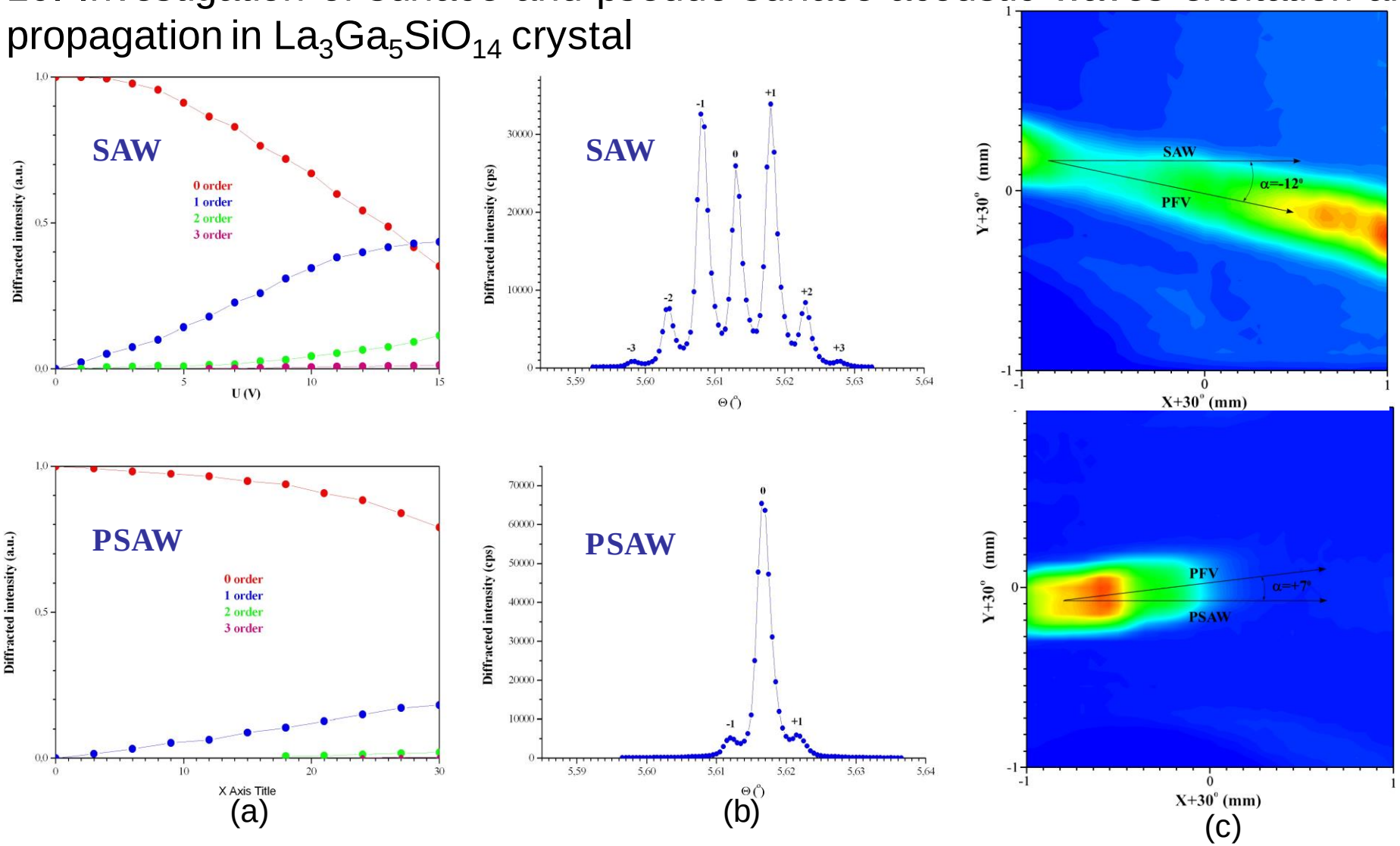

(a) (b) (c)

X-ray diffraction by the *Z*-cut of an LGS crystal modulated by a SAW (SAW propagation along (*X*+30°) direction): (a) dependences of the intensities of the diffraction satellites versus amplitude of the input signal supplied to the IDT; (b) rocking curves measured at amplitude of the input signal U=15 V; (c) 2D map of the distribution of the diffracted X-ray radiation on the crystal surface. (001) reflection; Θ_B=5.619º. The resonance frequency of Λ=6 µm SAW excitation was *f*=416 MHz, which corresponds to SAW velocity of ***V*=2496 m/s**, while in the case of PSAW excitation the resonance excitation frequency is *f*=496 MHz at the velocity of ***V*=2976 m/s**.

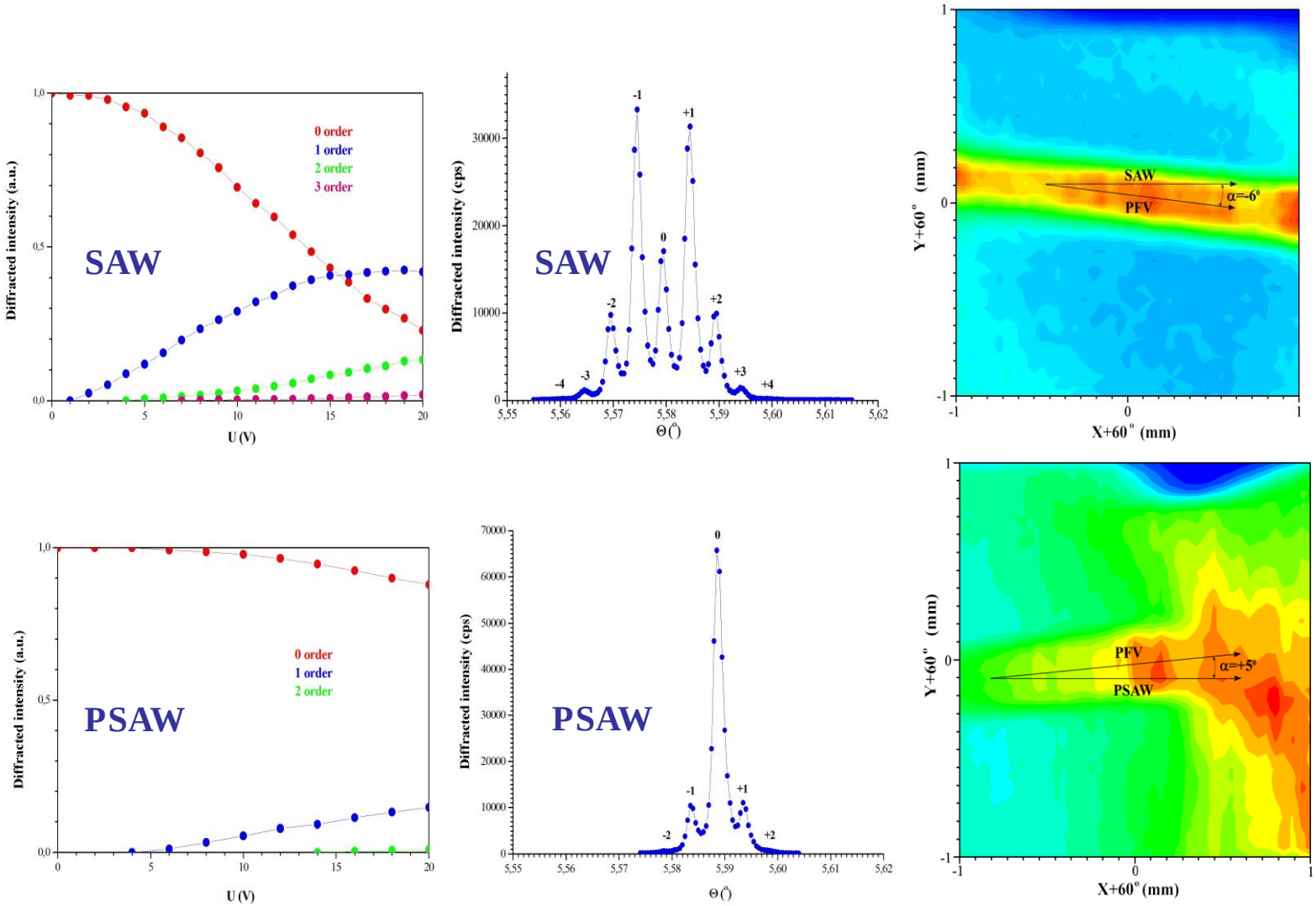

(a) (b) (c)

X-ray diffraction by the *Z*-cut of an LGS crystal modulated by a SAW (SAW propagation along (*X*+60°) direction): (a) dependences of the intensities of the diffraction satellites versus amplitude of the input signal supplied to the IDT; (b) rocking curves measured at amplitude of the input signal U=20 V; (c) 2D map of the distribution of the diffracted X-ray radiation on the crystal surface. (001) reflection; Θ_B=5.619º. The SAW with wavelength of Λ=6 µm was excited at resonance frequency *f*=396 MHz and propagated on the crystal surface with a velocity of ***V*=2376 m/s**. The PSAW was excited at resonance excitation frequency *f*=516 MHz and propagated with a velocity of ***V*=3096** m/s.

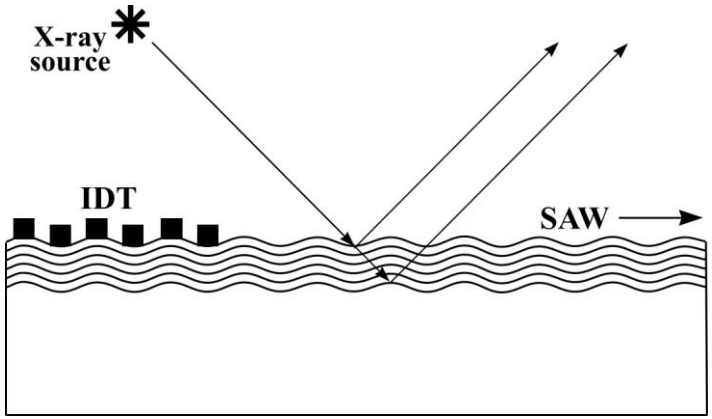

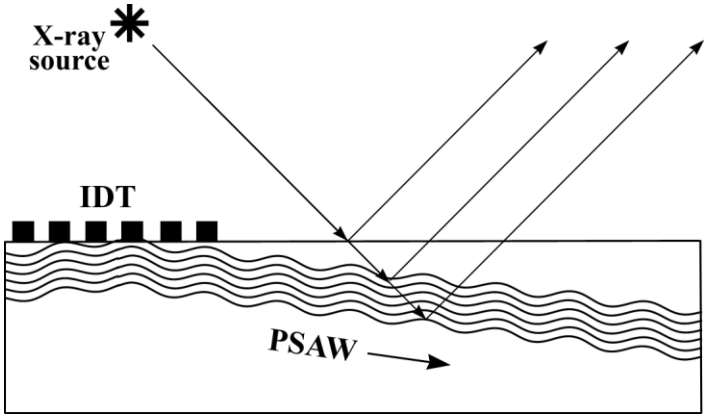

Schemes of the SAW and PSAW propagation in the Z-cut of an LGS crystal

Thanks for your attention!